

FORMABILITY OF SHEET METAL.

JOSEPH YING FAN LIN

A MAJOR TECHNICAL REPORT

in  
the Faculty  
of  
Engineering

Presented in Partial Fulfillment of the Requirements for the  
Degree of Master of Engineering at  
Sir George Williams University  
Montreal, Canada

August, 1973

FORMABILITY OF SHEET METAL

BY

JOSEPH YING FAN LIN

ABSTRACT

The principal mechanical parameters useful for predicting the formability of sheet metal are reviewed.

A manufacturing analytical technique is available for the study of formability in sheet metal stamping which involves the complex combinations of deep-drawing and stretching operations commonly applied in industry. A plot of the maximum and minimum principal surface strains at failure on a sheet metal pressing results in a Forming Limit Diagram (FLD). The strains are measured by means of a grid applied to the sheet metal surface prior to stamping. A FLD can be prepared for each new stamping and used to monitor operating variables, evaluate die modifications and establish material specifications to achieve a satisfactory stamping in the press shop.

The interactions of material properties, part design, punch and die design and pressing conditions are such that many factors must be considered in assessing sheet metal formability. The influences of material properties on forming are examined, especially the correlations of work-hardening exponent and anisotropy coefficient with press performances. Stamping is also affected by punch and die design, lubrication, surface roughness and other press operating variables.

#### ACKNOWLEDGEMENTS

I wish to express my gratitude and deep appreciation to my supervisor, Professor Hugh J. McQueen, for providing his valuable advice, criticism and encouragement throughout the course of this study.

In the preparation of this work I was fortunate to have the interest and assistance of many individuals. To all of them go my sincere thanks. I am particularly indebted to Miss M. Bradley and Mrs. M. Mendonca, who typed the entire manuscript.

My appreciation is to my wife, Bess, for proof-reading the entire manuscript and most of all, for her patience and understanding. Everlasting gratitude to my Father who, with great difficulties, provided my university undergraduate education.

## TABLE OF CONTENTS

	PAGE
I INTRODUCTION . . . . .	1
1.1 Forming of Sheet-Metal . . . . .	1
1.1.1 Deep-Drawing . . . . .	2
1.1.2 Stretching . . . . .	4
1.2 Relations of Fundamental Material Properties Tests with Press Performance . . . . .	5
1.2.1 Tensile Test . . . . .	5
1.2.2 Hardness Test . . . . .	7
1.2.3 Chemical Composition Analysis . . . . .	7
1.3 Attempts in Duplication of Press Performance by Simulative Tests . . . . .	8
II GRID ANALYSIS SYSTEM . . . . .	11
2.1 General . . . . .	11
2.2 Gridline Spacing (Size of Pattern) . . . . .	11
2.3 Gridline Configuration and Orientation . . . . .	14
2.3.1 Squares Pattern . . . . .	14
2.3.2 Circles Pattern . . . . .	16
2.3.3 Combination of Circles and Squares . . . . .	18
2.4 Gridline Marking Techniques . . . . .	18
2.4.1 Scribing Method . . . . .	20
2.4.2 Rubber Stamping and Silk Screening Methods . . . . .	20
2.4.3 Photographic Method . . . . .	21
2.4.4 Electrochemical Method . . . . .	22

	PAGE
2.5 Measurement of Grid Patterns and Strain Calculations After Stamping . . . . .	26
 III STRAIN ANALYSIS AND FORMABILITY LIMITS . . . . .	 29
3.1 General . . . . .	29
3.2 General Low Strain Distribution . . . . .	30
3.3 Critical Strain Distribution . . . . .	30
3.4 Strain Histories . . . . .	31
3.5 Forming Limit Diagram (FLD) . . . . .	35
3.5.1 Critical Strain Level Curve (Keeler-Goodwin Curve) . . . . .	35
3.5.2 Definition of the Criterion for Failure for the Critical Strain Level . . . . .	39
3.5.3 Factors Affecting the Critical Strain Level . . . . .	42
3.5.4 Use of the Forming Limit Diagram (FLD) . . . . .	46
 IV STANDARD MECHANICAL PROPERTIES AFFECTING STRETCHABILITY AND DRAWABILITY . . . . .	 54
4.1 General . . . . .	54
4.2 The Work-Hardening Exponent (n) . . . . .	54
4.2.1 Methods for Evaluating the n value . . . . .	58
4.2.2 Factors Influencing Work-hardening Exponent . . . . .	64
4.2.3 Effect of Work-hardening Exponent on Stretching . . . . .	66
4.2.4 Effect of Work-hardening Exponent on Deep-drawing . . . . .	74
4.3 Plastic Anisotropy Coefficient (Strain Ratio), r . . . . .	74
4.3.1 Method for Determination of the Strain Ratio . . . . .	76
4.3.2 Planar Anisotropy Coefficient ( $\alpha_r$ ) . . . . .	80
4.3.3 Normal Anisotropy Coefficient ( $\bar{r}$ ) . . . . .	81
4.3.4 Isotropic Material . . . . .	83
4.3.5 Factors Influencing Anisotropy . . . . .	84
4.3.5.1 Mechanical Fibering . . . . .	87
4.3.6 Effect of Anisotropy on Deep-drawing . . . . .	87
4.3.7 Effect of Anisotropy on Stretching . . . . .	94
4.4 Correlation of Stamping Performance of Sheet-Metal with Work-hardening and Anisotropy Properties . . . . .	95

	PAGE
V EFFECTS OF VARIABLES AND APPLICATION OF FORMING LIMIT DIAGRAM ON THE IMPROVEMENT OF FORMABILITY . . . . .	98
5.1 General Approach for Satisfactory Stamping . . . . .	98
5.2 Characteristics of Material Affecting Stamping . . . . .	101
5.2.1 Influences of Yield Stress . . . . .	102
5.2.2 Disadvantage of Yield-Point Elongation . . . . .	102
5.2.3 Effect of Grain Size . . . . .	103
5.2.4 Effects of Prior Cold Work . . . . .	103
5.2.5 Effect of Strain Aging . . . . .	104
5.2.6 Effects of Surface Scratch or Subsurface Lamination and Burr . . . . .	105
5.2.7 Advantages of Coating on Metal Blank . . . . .	108
5.3 Effect of Forming Radius in Part Design . . . . .	109
5.4 Influences of Press Operating Conditions . . . . .	110
5.4.1 Effects of Lubrication and Friction . . . . .	110
5.4.1.1 Lubrication in Deep-Drawing . . . . .	113
5.4.1.2 Advantage of Lubrication in Stretching Over a Large Radius Punch . . . . .	114
5.4.1.3 Advantage of Friction in Stretching Over a Small Radius Punch . . . . .	115
5.4.1.4 Effect of Blank Surface Roughness . . . . .	116
5.4.2 Effects of Pad or Blankholder Pressure . . . . .	116
5.4.3 Effects of Punch Forming Speed . . . . .	117
5.4.4 Problems in Multistage Forming Operations . . . . .	118
VI CONCLUSIONS . . . . .	120
REFERENCES . . . . .	121

## NOMENCLATURE

BCC	body-centered cubic metal
FCC	face-centered cubic metal
FLD	Forming Limit Diagram
HCP	hexagonal close-packed metal
K	constant
LDR	Limiting Drawing Ratio
P <sub>u</sub>	maximum load
P <sub>10</sub>	load at 10 percent strain
RSF	Relative Safety Factor
UV	ultra-violet
W <sub>f</sub>	final width
W <sub>o</sub>	initial width
a.c.	alternating current
d.c.	direct current
e <sub>1</sub>	maximum (major) principal surface strain
e <sub>2</sub>	minimum (minor) principal surface strain
e <sub>w</sub>	engineering width strain
e <sub>t</sub>	engineering thickness strain
k	constant
l	real length of the axis of the deformed grid-circle
l <sub>f</sub>	final length
l <sub>o</sub>	initial length
n	work-hardening exponent (work-hardening coefficient)
r	plastic anisotropy coefficient (strain ratio)

$\bar{r}$	normal anisotropy coefficient
$\Delta r$	planar anisotropy coefficient
$r_o$	strain ratio in the rolling direction
$r_{45}$	strain ratio at 45 degrees to the rolling direction
$r_{90}$	strain ratio at 90 degrees to the rolling direction
$t_f$	final thickness
$t_o$	initial thickness
$\alpha$	angle between the metal surface and the plane perpendicular to the optical axis
$\Delta$	error in measurement
$\varepsilon$	true strain
$\varepsilon_T$	true thickness strain
$\varepsilon_W$	true width strain
$\varepsilon_u$	maximum uniform elongation
$\sigma$	true stress
$\sigma_1 \sigma_2 \sigma_3$	principal stresses

CHAPTER 1  
INTRODUCTION

**1.1 FORMING OF SHEET-METAL**

The aim of sheet-metal forming is the production of satisfactory parts by plastic deformation of sheet-metal. The capacity of a metal to undergo forming without failure through fracture is the formability. This quality is elusive to measure as there is no single index that will enable its reliable prediction for any production condition or stamping. A material that is readily formable for one stamping design may break when it is used for a stamping having a different configuration. The forming load required to make a pressing is usually well within the press capacity; it is the ductility of the metal which limits the process. Whether the ductility can be utilized to the greatest advantage will depend upon the surface condition of the metal and the tools, the blank shape, the applied blank-holder pressure, speed of forming, lubrication and frictional effects, tool and part design, etc.

The word stamping is used to cover all of the operations required to form a flat sheet into a part. These operations may include deep-drawing, stretching, bending, buckling and others. In most production parts, deformation takes place by a combination of deep-drawing, bending and stretching. The relative amounts of stretching and drawing vary from stamping to stamping, or even at different locations within a stamping. The properties of a

material required for good stretchability are not the same as those that impart good drawability.

As stamping is cheap and readily adapted to a large-scale production, it is used widely, especially by those industries producing automobile bodies, household electrical appliances and a variety of small utensils.

Stampings which serve a decorative purpose rather than a structural are acceptable only if there are no obvious tears, wrinkles, cracks or necks in the finished stampings. In areas of highly localized strain, the surface of the metal sheet may become roughened which is objectionable if it is exposed in the end product, especially if it is plated. Other stampings which serve mainly a structural purpose, require strength and ductility in the finished condition. Examples are the frame members of automobiles, propane tanks, fire extinguisher cylinders and side panels of monocoque automobile bodies.

#### 1.1.1 DEEP-DRAWING

Deep-drawing, cup drawing or radial drawing, is a process whereby a blank sheet-metal is converted into a flat-bottom cylindrical cup. (2,14,19,28,33,34,35) The blank, which may be circular, rectangular, or of a more complex outline, is drawn into the die cavity by the pressure of a punch, as shown in Figure 1.1.

No deformation occurs under the bottom of the punch, the area of the blank originally within the die opening. As the punch forms the cup, the flange moves into the die opening becoming the cylindrical shell through radial extension coupled with circumferential shrinkage.

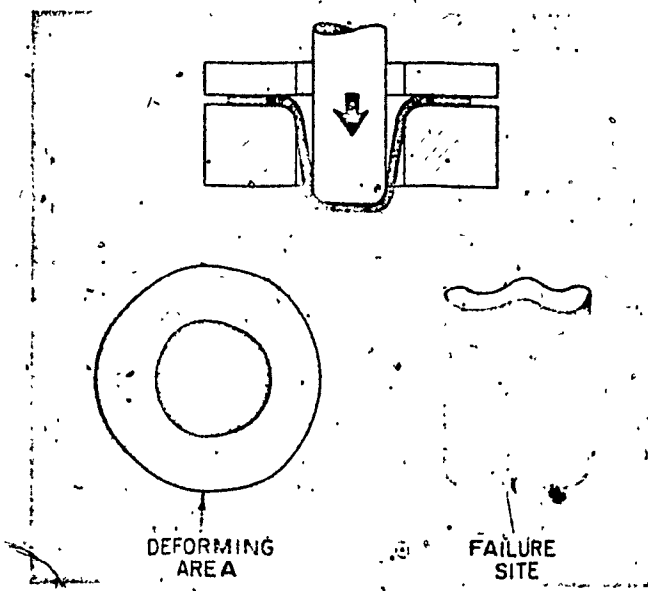


Figure 1.1. Deep-drawing Operation. (From Ref. 2, 33)

In deep-drawing, the limit of deformation is reached when the load required to deform the flange becomes greater than the load-carrying capacity of the un-worked area near the bottom of the cup wall. Hold-down pressures and friction in bending and unbending over the die radius influence the deformation limit. Unwanted buckling or wrinkling of the flange is due to excessive hoop compressive stress induced in the flange. They can be minimized by decreasing the yield stress of the metal, raising the hold-down pressure, reducing the clearance between punch and die, increasing the thickness of the blank, or reducing its diameter.

The formability in deep-drawing is specified by the Limiting Drawing Ratio (LDR) which is defined as the ratio of the maximum blank diameter that can be drawn into a cup without failure to the diameter of the die. (7,14,33)

Examples of deep-drawing parts are automotive oil pans, hydraulic pump housings, propane cylinders, vegetable pans for refrigerators and bathtubs.

#### 1.1.2 STRETCHING

In stretching, illustrated by Figure 1.2, the flange of the flat blank is securely clamped. Biaxial extension which can be characterized as radial extension with no circumferential shrinkage, (2,14,33,34) is restricted to the area initially within the die. The stretching limit is the onset of tearing. Location of the failure depends on the material and the forming conditions.

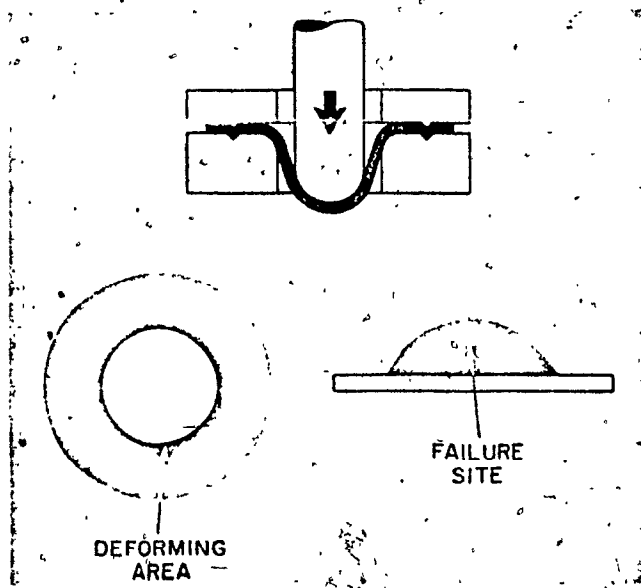


Figure 1.2. Stretch Forming Operation, (From Ref. 2,33)

## 1.2 RELATIONS OF FUNDAMENTAL MATERIAL PROPERTIES TESTS WITH PRESS PERFORMANCE

The causes of failure in complex pressings are many, and neither the engineer nor the metallurgist has been wholly successful in correlating press performance with mechanical properties obtained from fundamental tests; such as tensile test, hardness test, micro-examinations, chemical analysis, etc. In fundamental tests, the three dimensional strain states imposed are quite different from the complex strain states applied in the forming of complex pressings.

### 1.2.1 TENSILE TEST

Some of the simple plastic properties measured in a tensile test are of use in evaluating the formability of sheet metal. The yield stress indicates the forces to be expected, however, the experimental value is usually lower than encountered in practice since the strain rates in tensile tests are considerably lower. Since necking is usually considered as failure, the uniform strain up to the ultimate tensile strength is a measure of the expected ductility. Total elongation is not satisfactory since it includes both uniform elongation and elongation after necking and is dependent on the gauge length over which the measurement is made. The ratio of tensile strength to yield stress is a good measure of the ability of a

metal to resist necking.

However, deep-drawing quality steel sheet is a very subtle material and methods must be devised to test the sheet under conditions of stress and strain similar to those existing in real processes. In any pressing operation, the material is subjected to two perpendicular stresses in the plane of the sheet and not just one as in the simple tensile test. The second or transverse stress affects the levels of stress at which the material yields and deforms and this is represented by the 'yield locus' in a stress diagram (Figure 1.3). This curve or locus is a fundamental property of the particular sheet and it shows the relationship between the two principal stresses at which the material yields. In a simple tensile test, one determines the point A on the locus and if the properties of the sheet are uniform in all directions, this would be sufficient to define the whole curve. Sheet-metal however, is never isotropic and its strength depends on the direction in which it is tested. This anisotropy results in a distortion of the yield locus which greatly affects the way the sheet-metal behaves in a pressing. Thus, one must perform tests under different ratios of combined stresses.

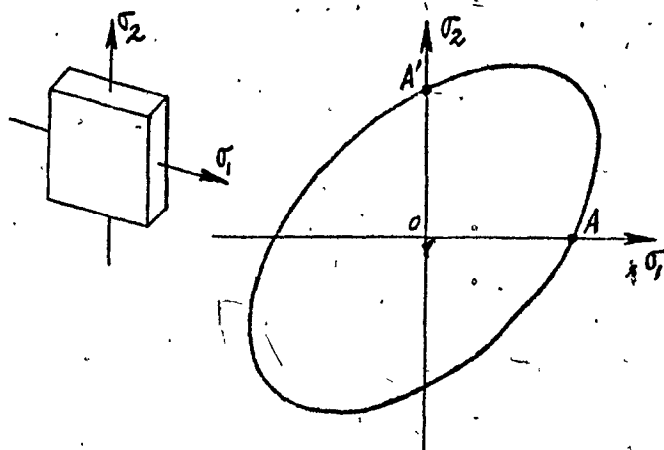


Figure 1.3. Stress diagram showing yield locus. Insert shows the principal stresses  $\sigma_1$  and  $\sigma_2$  on an element of the sheet ( $\sigma_3=0$ ).

#### 1.2.2 HARDNESS TEST

Since the hardness test approximately measures flow stress at 8% strain, it can give an indication of the forces needed for pressing but gives no information about the formability.

#### 1.2.3 CHEMICAL COMPOSITION ANALYSIS

Most steel stampings are made from low carbon steels which contain from 0.02 to 0.08 percent carbon, plus varying amounts of aluminum, silicon, manganese, nickel, chromium and other elements. Although minor variations in chemical contents can affect the formability of sheet metals, other factors in the processing of the strip can completely overshadow them.

### 1.3 ATTEMPTS IN DUPLICATION OF PRESS PERFORMANCE BY SIMULATIVE TESTS

In an attempt to duplicate more closely actual forming operations, a series of simulative tests have evolved within the forming industry. Examples of these tests include the Erichsen, Olsen, Fukui, Swift and hydraulic bulge tests. Problems encountered with these tests include:- scale effects, edge effects, types of lubrication, speed of deformation and test equipment standardization. These and other test procedures often influence the results obtained as much as the material itself.

Even if testing problems could be eliminated, there remains a basic obstacle to correlation of press performance data with fundamental and simulative test results. A stamping operation is composed of various combinations of stretch and draw, to which bending, buckling, and other complications are added. One could imagine a particular stamping to have a specific combination within the broad spectrum, as indicated by the arrow in Figure 1.4. Each of the fundamental and simulative tests can also be positioned along this spectrum. (13,28,29,30,32,33,36) It is easy to understand why a formability test correlates with the press performance data of certain stampings and yet have no correlation with other stampings.

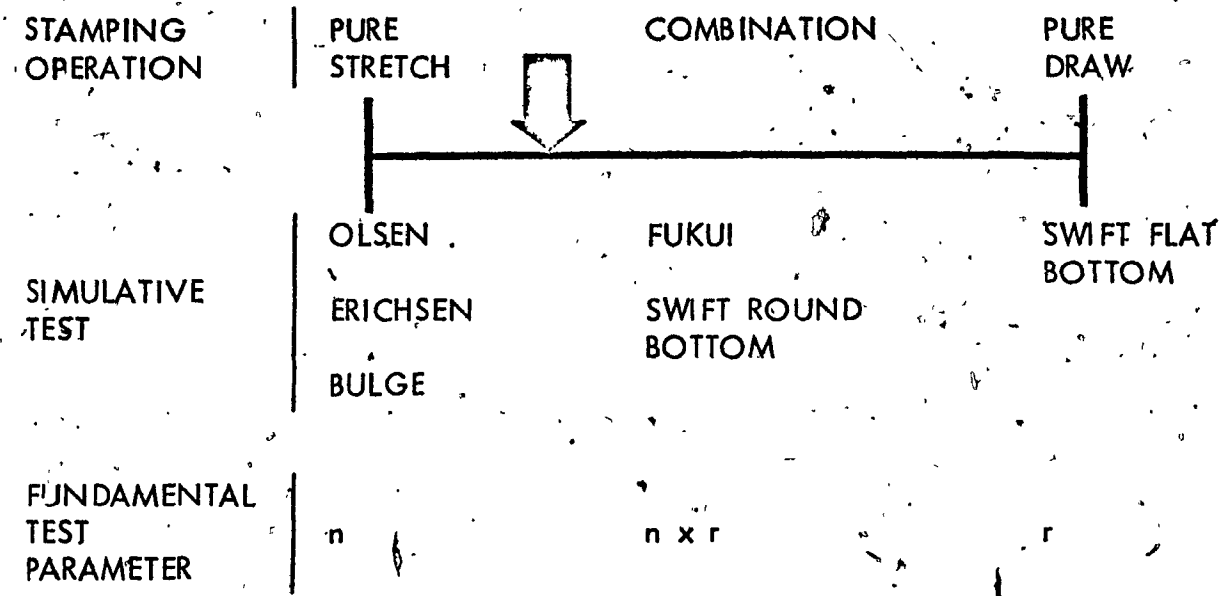


Figure 1.4. Schematic of complex stamping formed by combination of stretch and draw.  $n$  and  $r$  are described in Chapter 4. (From Ref. 36)

Good correlation between press performance and material property data can be obtained if the relative amounts of stretch and draw in each are matched. These amounts are not generally known except for some extreme cases, such as deep drawn cups and hydraulically bulged domes. Additionally, the exact position of a stamping within the spectrum varies with material properties, surface roughness, lubrication, blank size, die and punch radii, press speed, etc. To further complicate the problem, each location in a complex stamping not only experiences different amounts of stretch and draw, but the relative amounts change with depth as the stamping is formed.

The correlation techniques for fundamental and simulative tests are sometimes successful if data are collected and analyzed over

long runs. This, unfortunately, is not very useful during die try-out periods or initial runs. The solution to the problem must be a technique which will quickly and accurately measure the ability of a single blank with given material properties to be formed into a specific stamping under the influence of the existing states of press and tool variables. This can be achieved by applying the grid strain analysis system.

CHAPTER 2  
GRID ANALYSIS SYSTEM

**2.1 GENERAL**

The amount of deformation before failure determines the sheet-metal formability. Since the strain in the thickness direction is negligible, the principal strains which develop in sheet-metal stamping can be studied through measurement of the surface strains.

This is done by imprinting the sheet-metal blank with a precise gridline pattern, which is measured after forming.

**2.2 GRIDLINE SPACING (SIZE OF PATTERN)**

Proper spacing between the gridlines is extremely important (14, 21, 22, 25, 28, 33, 36) and the choice is governed by a number of factors, namely; the purpose for which the workpiece is gridded, the geometry of the part, the strain gradient anticipated and the required accuracy. Since all the material between adjacent grid-lines is considered as one unit, any variation in strain from point to point between the lines is undetectable; only an average strain value is obtained. Therefore, grid spacings must be sufficiently small to provide accurate determination of peak strains and measurement of the very localized differences in strain distribution. The diameter of the circles currently used vary from 0.05 to 0.25 inch, depending upon the

strain gradient. For flat areas of large roof, hood, door and quarter panels with relatively constant strain levels, a diameter of 0.25 inch is satisfactory. For areas bent over sharper radii or punch heads and for general applications, 0.10 inch diameters are more applicable. Some very critical and sharp radii require 0.05 inch diameter circles for accurate evaluation of the peak strain.

To illustrate the primary disadvantage of large grid spacings or strain measurements, the strain distribution obtained with a grid pattern of 0.10 inch spacings oriented parallel to the principal strain direction is shown in Figure 2.1 for an automotive bumper stamping. (21,28,33) Parts A and B were formed before and after an experimental modification, which caused substantial differences in the peak strains. The same maximum peak strains calculated for larger and larger grid spacings are plotted in Figure 2.2. The 'A max.' values were obtained by locating the strain peak in the centre of the grid spacing, while the 'A min.' curve was obtained by placing the peak strain at one edge of the grid spacing. Evidently, measured strain, then, is very dependent on gridline spacing (gauge length). The larger the gauge length, the more the peak strain is averaged with lower strains. Furthermore, for any given grid spacing, the maximum and minimum curves indicate the range of values which could be obtained on this stamping by random placement of the grid. As an example, the range for a 0.50 inch gauge length shown in Figure 2.2 for part A is 29 per cent to

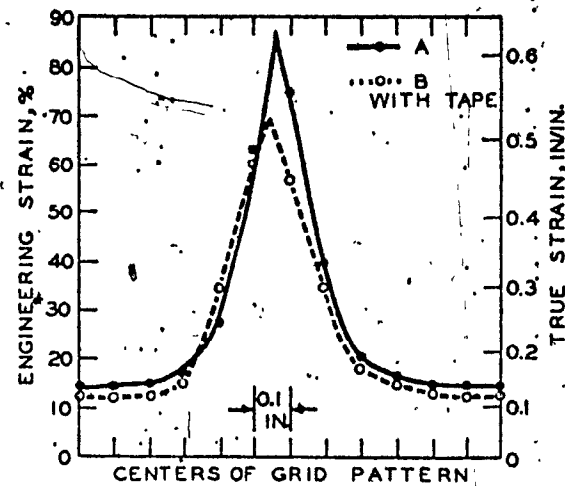


Figure 2.1. Distribution of principal strain across an area of biaxial stretch in a production automotive bumper. Stamping A was produced by usual production methods. Stamping B had emery tape placed on the punch at the high strain region to restrict metal flow. Both stampings had fractured. All measurements are plotted at the centre positions of the undeformed 0.10 inch diameter grid circles. (From Ref. 28, 33)

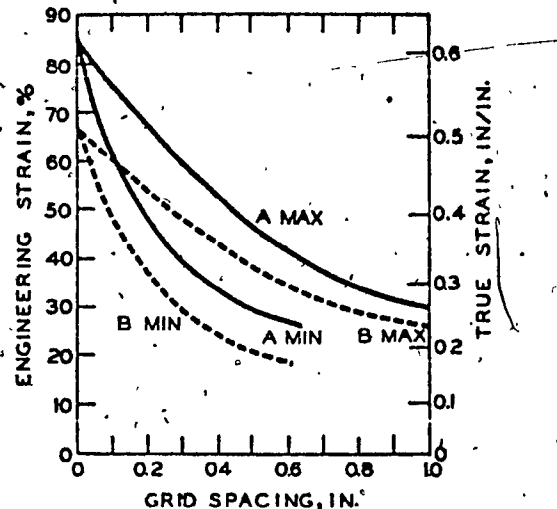


Figure 2.2. Calculated average strain plotted against grid size for a strain distribution measured in a production automotive bumper. Curve was extrapolated to zero grid size. (From Ref. 28, 33)

47 percent, while part B has a range of 21 percent to 38 percent.

Therefore, depending on the placement of a 0.50 inch grid, the strain of part B might be less than, equal to, or greater than part A.

### 2.3 GRIDLINE CONFIGURATION AND ORIENTATION

The several types of gridline patterns presently in use include circles (interlocking, touching or not touching arranged in rows); squares or combinations of circles and squares.  
(14,21,22,25,33,36,37)

#### 2.3.1 SQUARES PATTERN

An early type of gridline pattern was composed of longitudinal and transverse parallel lines which form squares on the sheet-metal blank. After the blank is formed, the square showing maximum deformation is used to establish the sheet-metal quality, often the increase in area is measured and calculated.

The configuration and orientation of the gridline pattern influences the measured strain values. (14,21,28,33,36)

The squares are seldom oriented to indicate directly the magnitude and direction of principal or maximum strain, these can be computed from the elongation and shear distortion of the square. This requires a considerable amount of work for an unsymmetrical stamping in which the principal strain directions change from point to point, while the direction of the grid system remains fixed.

The difficulty with squares pattern can be illustrated in Figure 2.3. When the sides of the square are oriented parallel to the direction of maximum elongation, the square will elongate into a rectangle. Simple measurements of the old and new dimensions permit calculation of the strain.

Again if the diagonals of the square are oriented in the direction of maximum elongation, the diagonal lengths of the old and new dimensions can be used to calculate strain. However, when the sides of and diagonals are oriented in other directions, the squares are very difficult to analyze.

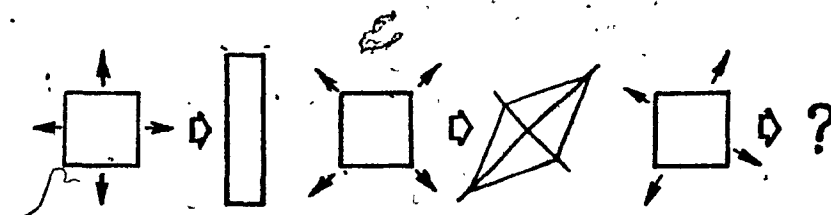


Figure 2.3. The disadvantage of square grid pattern.  
(From Ref. 25, 33)

The squares have been used in the past because they can be conveniently scribed by intersecting sets of parallel lines. Furthermore, the square pattern did provide a starting point from which the system of gridline analysis evolved.

### 2.3.2 CIRCLES PATTERN

An ideal gridline system is non-directional; this is fulfilled by circles which have a major advantage over squares. (14, 21, 22, 25, 28, 33, 36, 37) The circles are always correctly oriented to furnish the maximum strains directly. When the sheet is deformed, the directions of the maximum strains are clearly displayed in the resulting ellipses; the magnitudes of principal strains may be calculated directly from measurements of the major and minor axes of the ellipse.

The choice of circle pattern is a matter of individual preference. Four common patterns are illustrated in Figure 2.4. Close-packed circles in pattern A have spaces between them which are not encompassed by grid elements. Butting circles in pattern B tend to have wide lines at junction points making measurements more difficult; open space also occurs in this pattern. The overlapping circles of pattern C are popular because all

of a given area is included in at least one circle; however, some areas are duplicated in measurements which could influence strain distributions - additionally, visualization of individual circles is difficult. The double overlapping in pattern D provides cross marks which act as locators for the centres of the circles and avoids wide lines at junction points. However, the pattern is overly complex, making it hard to visualize strain.

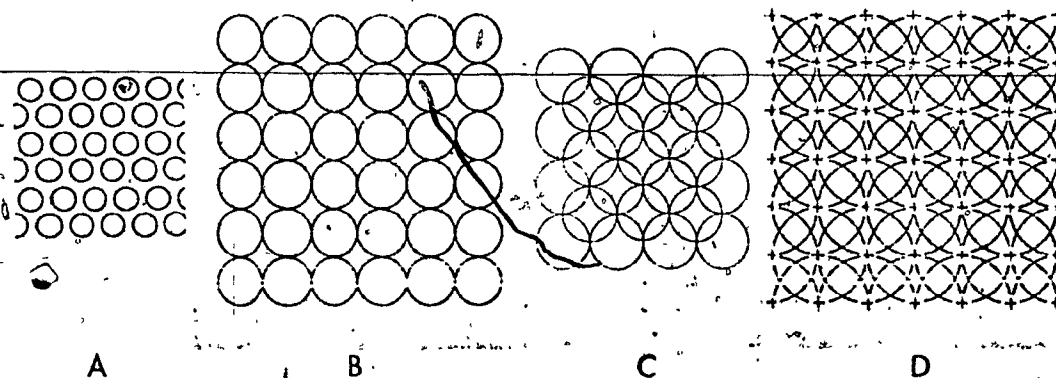


Figure 2.4. Typical circle patterns used in formability studies: A, Close-packed; B, butted; C, overlap; D, double overlap.  
(From Ref. 21, 22, 33, 36).

In the case of circle grids covering relatively large areas on complex pressings, it is not always possible to easily identify the origin of specific circles.

### 2.3.3 COMBINATION OF CIRCLES AND SQUARES

In the grid consisting of circles and parallel lines (Figure 2.5), the parallel lines are not used in strain measurements. They are aids in identifying a particular row of circles or an individual circle and in evaluating flow lines throughout the stamping. However, there are spaces between circles which are not encompassed by the pattern. No strain measurements are made in the spaces between the circles. (21, 33, 36)

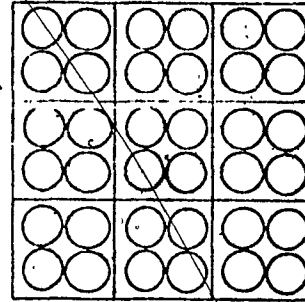


Figure 2.5. Circles-in-Squares Pattern. (From Ref. 21, 22, 33, 36).

### 2.4 GRID-LINE MARKING TECHNIQUES

A number of techniques are available for applying grids. Comparison of these techniques was made by Branson (21) and is reproduced in Table 2.1. At present the electrochemical etching process appears to be the most generally preferred method for applying grids since it is accurate, quick and easy to use.

Table 2.1. Comparison of gridline marking techniques. (From Ref. 21)

	Scribe	Rubber stamp	Silk screen	Photogrid	Electroetch
<b>Main advantages</b>	flexible	quick	quick, fairly accurate, easy line width and thickness	extreme accuracy	quick, accurate, easy
<b>Main disadvantages</b>	Inaccurate, too deep	limited accuracy	unlimited	time and equipment	power source
<b>Size of blank</b>	unlimited	unlimited	unlimited	3ft by 3ft	unlimited stencil
<b>Master pattern</b>	none	stamp	photographic silk screen	negative	
<b>Type of pattern</b>	generally lines	any	any	any	
<b>Depth of mark</b>	slight to very deep	+ ink thickness — etch depth	+ ink, lacquer, or enamel thickness	+ coating thickness	$\pm 0.01\text{in}$
<b>Pattern limits</b>	ability to layout	limited by resolution	none	none	none
<b>Resolution</b>	unlimited	limited—coarse	slightly limited	unlimited	slightly limited
<b>Accuracy</b>	poor	good	good	excellent	very good
<b>Reproducibility</b>	poor	good	good	excellent	excellent
<b>Adherence</b>	excellent	poor for ink, excellent for etch clean	poor to excellent	good	excellent
<b>Surface preparation</b>	none	solvent clean	acid cleaning	solvent clean	
<b>Equipment required</b>	rule and scribe	stamp	UV light, negative, source	key coating	power source, electrode, stencil
<b>Chemicals required</b>	none	ink or plating	photosensitive coating developer	none	electrolyte, sometimes neutralizer
<b>Portability</b>	extremely easy	extremely easy	good	30min +	excellent—depends upon power source 2min
<b>Speed per unit area</b>	very long	30sec	2min to 2hr	30min +	

#### 2.4.1 SCRIBING METHOD

Early methods of producing gridlines involved the use of hardened steel or diamond tool to hand or machine scribe straight lines and produce squares, (33,36,37) however it is difficult to produce accurately small squares on a piece of metal. With the advent of grids composed of circles, the difficulties of scribing such patterns increased enormously. Use of a numerically controlled machine to scribe the requisite grid pattern offers an accurate means of marking. (37) However, since a grid may typically involve some 3,000 linear inches of marking, even with a tool speed of 1 inch per second, the scribing will still take upwards of an hour. The machine time and the necessary control tape are relatively expensive.

Scribed pattern has another disadvantage - the lines can introduce stress concentrations as evidenced by failure along scribed lines. (33,36) Consequently, the strain pattern is inaccurate.

#### 2.4.2 RUBBER STAMPING AND SILK SCREENING METHODS

The first attempt at creating a rapid application method of grid marking involved the use of a rubber stamp and marking ink. (28,33,36,37) However, resolution and

accuracy of the grid are limited, and the ink markings are easily erased or smudged during stamping. The ink can be replaced by copper plating solution or by acid etchants. These produce broad lines so measuring accuracy is poor.  
(2,33)

Fine lines can be applied through silk screen masters. The imprinting and drying are slow. (33)

#### 2.4.3 PHOTOGRAPHIC METHOD

For laboratory tests, the photographic method provides very fine and accurate grid systems, such as 100 lines to the inch. The sheet-metal blank is coated with photosensitive emulsion. The gridlines are produced by contact exposure with a master photographic negative and by developing like a photographic print. (2,28,31,33,36,37) The time to produce one grid can be greater than 30 minutes, and special equipment and darkroom are required. Therefore, the technique is generally limited to small parts which are being evaluated in the laboratory. (28,31,33,36)

One deficiency of these grids is their easy removal by rubbing over the die. This problem of erasure has been overcome by using a photosensitive polymer emulsion which serves as a mask for etching the metal by chemical treatment, in much the same way as printed circuits boards are

prepared. This technique, however, increases the preparation time to well in excess of an hour, to which is added the trouble of removing the polymer layer from the blank. The laboratory of Hoogovens (Germany) has used electrochemical methods to etch out on the metal surface to give greater resistance against rubbing off. (31)

#### 2.4.4 ELECTROCHEMICAL METHOD

The electrochemical marking technique for producing grid-line patterns which is schematically shown in Figure 2.6 is currently being used for shop formability tests, (14,21,22,25,28,31,33,36,37,39,40) A non-conducting fibrous sheet which is treated to make the lines forming the desired pattern conducting, becomes an electrochemical stencil. This stencil is placed on the cleaned sheet-metal blank and covered with a felt pad soaked in electrolyte. One electrode is attached to the sheet and a weight which serves as an electrode, is placed on the felt pad and is firmly pressed against the surface. A 14-volt a.c. (or d.c.) current, generated by means of a power unit, is passed through the system for approximately 5 to 7 seconds. The amperage required is a function of total conducting area. An alternative technique permitting higher pressures and requiring less amperage, but more time utilizes a roller or rocker type electrode to

press on the felt pad. With either electrode, the gridline pattern is etched into the blank and a black deposit forms in the grid-lines. After etching, the solution on the blank is neutralized and oil is applied to prevent rusting.

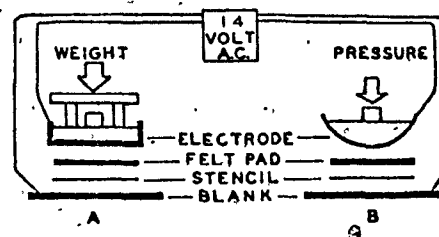


Figure 2.6. Schematic of electrochemical marking system:  
A, flat electrode requiring high amperage  
(200 amp. or more); B, rocker electrode for  
low amperage. (From Ref. 36)

The grid design produced is determined by the stencil which limits contact between the workpiece and electrolyte current to the desired pattern. (37) Stencils can be made of various materials and by various processes, depending to some degree on the accuracy required. (39) The accuracy, using the paper (impregnated with plastic material) stencil, of  $\pm 2\%$  is not unreasonable when one takes into account the variation in line thickness and line broadening which occurs during deformation. The accuracy and fineness of line produced by a woven nylon stencil (impregnated with plastic) appears to be limited by the fibre size in the cloth.

Sharp and distinct markings are produced, the nature of which depends on the type of current passed. (37) During each cycle of alternating voltage, metal is first etched from the metal blank and then re-deposited in the resulting cavity in the form of a black coherent compound which contrasts sharply with the base metal. The re-deposition ensures that the surface of the blank remains flush, avoiding the formation of cavities or ridges. With a direct current, metal is progressively etched from the blank without re-deposition, to produce a permanent depression which usually has a frosted-white appearance to the base metal. Alternating current is more frequently used and is applicable to the common ferrous and non-ferrous metal and alloys - whether plated, galvanized or untreated - with the exception of aluminum. Both aluminum and the foregoing metals and alloys may be marked by the d.c. etch. In the case of aluminum, the normal frosted-white etch may be pigmented black by the appropriate choice of electrolyte. (37)

The amperage need not generally exceed 25A, but power units up to 100A can be obtained for marking very large areas.

(21,25) The depth of the mark is proportional to the time of application and the current density; a depth of the order of 0.0001 inch can be produced in one second.

(36,37,39) Line sharpness is improved by short marking time, high current density and low uniform contact pre-

ssure consistent with sufficient line density. Overheating or excessive hydrogen evolution produces non-uniform or only partial marking and can also damage the stencils. (21)

Since the gridline pattern is etched, it cannot be removed by oil, chemicals or ordinary abrasion and rubbing of the material over the dies. (14,28,31,33,36,39) There are obviously no problems of adhesion of the mark in the d.c. case, and in a.c. case, the oxide adheres strongly to the metal even after cold rolling. (39) No evidence has been accumulated which would suggest that the electrochemical grid-mark causes premature failure in stamping and studies of fractures do not suggest that they initiate from a mark or propagate along them. (14,28,36,39) Further, a report on the effect of electro-marking on corrosion and fatigue behaviour of a range of aluminum alloys concludes that it does not adversely affect either of these properties. (39)

Since the equipment is portable, a grid may be applied rapidly at the press line on production size blanks. (14,28)

## 2.5 MEASUREMENT OF GRID PATTERNS AND STRAIN CALCULATIONS AFTER STAMPING

After forming is complete, the strains are measured from the distorted circles on the etched blank which generally take the shape of ellipses. Regardless of the strain state, the major axis of each ellipse is always parallel and proportional to the maximum principal strain in that part of the surface. From the minor axis, the magnitude and direction of the minimum principal surface strain can be obtained. (9,15) The major and minor axes of the ellipses are measured in numerous ways. (9,11,12,15,22,33,36) For rough measurements, simple flexible rules or calibrated plastic tapes are satisfactory. Higher accuracy is provided by using dividers and a rule calibrated in hundredths of an inch. For areas where there are sharp radii, use is made of a very flexible plastic scale ruled in hundredths of an inch which can fit over the sharp radii. (21) For more accurate measurements, an optical magnifier or microscope with a graduated graticule is used. A common error which arises when microscopes are used for measuring distorted circles on the deformed sheet surfaces, (21,31) arises when the metal surface is not perpendicular to the optical axis. This error is difficult to avoid, especially on complicated deformed surfaces. In Figure 2.7, the error ( $\Delta$ ) expressed in terms of the real length ( $l$ ), can be derived in a simple way:

$$\frac{\Delta}{l} = 1 - \cos \alpha$$

This type of error can be avoided by executing the measurements on replica foils. As the plane of the foil is always true with the optical axis, the real length of the distorted circle is obtained, regardless of the degree of sheet curvature. In the case of a curved surface, a correction for the curvature need only be applied for radii of less than about 0.1 inch. For radii in excess of this, the difference between the arc length and subtended chord length is small enough to be ignored. (21)

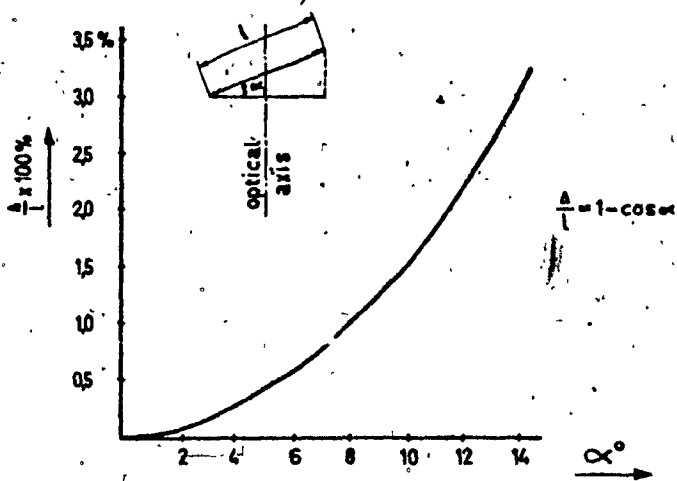


Figure 2.7. Error caused by angle  $\alpha$  (From Ref. 31)

In obtaining the lengths of both axes of the ellipse, the major and minor strains are calculated from the change in dimensions. (3,12,14,25)

Length of one of      Original Diameter  
Percent Strain = the axes of ellipse of Circle      X 100%  
                            Original Diameter of Circle

### CHAPTER 3

#### STRAIN ANALYSIS & FORMABILITY LIMITS

##### 3.1 GENERAL

When a stamping tears during forming, the sheet-metal has been worked beyond its formability limit. Recent research makes it possible to predict this failure and avoid forming problems.

Gridline patterns applied to the sheet-metal blank prior to forming into the stamping, have proved valuable in assessing the type and magnitude of the strain developed. Gridline marking provides several types of information, namely; a general visual pattern of metal flow, an indication of regions with critical strain distributions and strain histories throughout the stamping, and a means of detailed critical strain analysis involving the use of a forming limit diagram (FLD). (21,22,33,39)

An important feature in visual examination of the deformed gridline pattern is to study the overall metal flow of stamping in detail. A large proportion of stampings involve striking a delicate balance between tearing and wrinkling conditions and often it is possible to isolate a troublesome area and trace its cause visually. Although previously this was possible to some extent by a study of burnished 'bearing' areas, the extra detail of gridline marking has proved a real advantage during blank and die development. (22)

### 3.2 GENERAL LOW STRAIN DISTRIBUTION

An imperfect shape often resulting from uneven strain distribution can be a major cause of rejection in shallow 'skin' panels. By employing gridline patterns and taking regular measurements over the surface of a stamping, it is possible to build up contour diagrams which show clearly the distribution of zones of equal strain. (22) The flow patterns observed can then be related not only to die features but to variables such as lubrication and material properties.

### 3.3 CRITICAL STRAIN DISTRIBUTION

In a critical area of a stamping the strain distribution exhibits maxima in progressive stages of forming prior to actual occurrence of localized necking. (27,31) The strain gradients at maxima are equal to zero. The schematic representation of some several stages of the strain distribution in a critical area is shown in Figure 3.1.

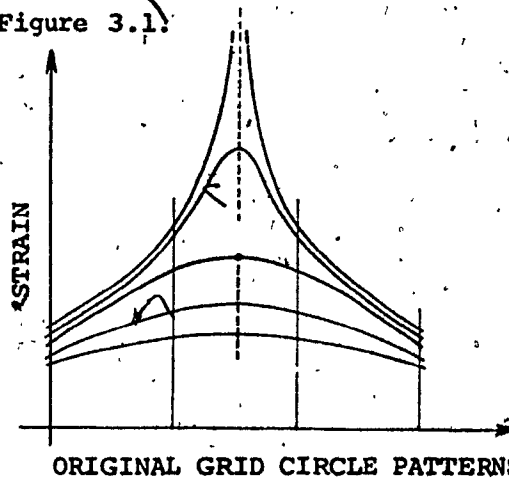


Figure 3.1 Strain distribution over three grid circles.  
(From Ref. 27)

### 3.4 STRAIN HISTORIES

Strain patterns in finished stampings can yield much useful information. However, the strain history in different areas of the stamping reveals how the high strain values built up and indicates the needed modifications in die design. The strain history of any desired location in the stamping can be obtained by stopping the punch at various progressive incremental stages of its descent, removing the partially formed stamping, and measuring the grid deformation. (14,28,33,37) The history of strain level is shown as a function of the depth of the stamping. Most deformation of interest usually occurs during the final 20 percent of punch travel. The strain histories should be obtained under conditions that approximate actual forming conditions as closely as possible since material properties and the effectiveness of lubrication are sensitive to deformation speed.

Examples of the history of strain distributions generated in an area of a stamping are presented here. Figure 3.2 shows the history of biaxial stretching at the 'nose' region of the punch in a typical automotive stamping. (28) As the depth of the stamping increases, all areas continue to strain. However, the strain rapidly concentrates at the previous high-strain location and the strain distribution becomes increasingly non-uniform or the gradient becomes steeper. If the stretching limit of the material is reached, the stamping tears.

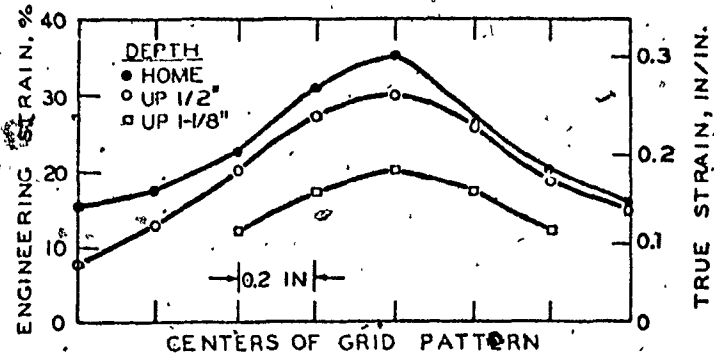


Figure 3.2. History of principal strain distribution across an area of biaxial stretch in a rimmed drawing quality steel automotive fender. All measurements are plotted at the centre positions of the undeformed 0.2 inch diameter grid circles. (From Ref. 28):

Figure 3.3 shows another similar example.<sup>(33)</sup> The strain distribution indicates a characteristic small amount of non-uniformity at 2.5 inches of punch travel. As the stamping is progressively formed, the general strain level increases. The degree of non-uniformity or amount of peaking increases with increasing depth. The completed depth is 6.8 inches.

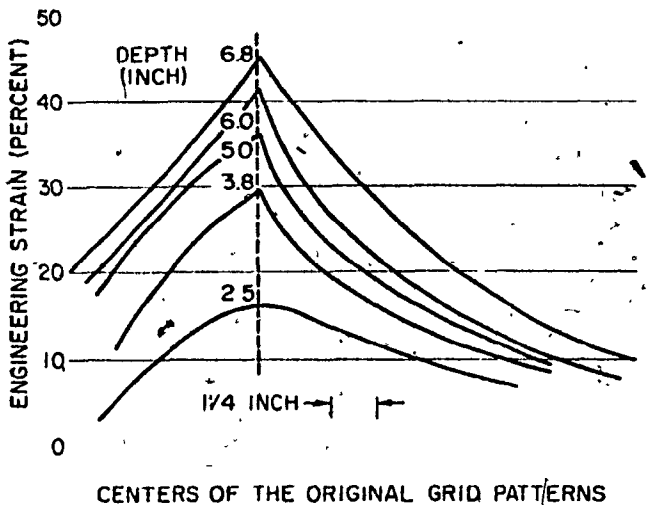


Figure 3.3. History of strain distributions across an area of biaxial stretch in the tail-light area of an automotive quarter-panel made with rimmed drawing quality steel. (From Ref. 33)

Using punch travel as the reference base, the strain history is obtained by cross-plotting the strains as a function of stamping depth. The strain history of this tail light area, as well as the bumper area of the same quarter-panel, is shown in Figure 3.4. (14,28,33) Examination of the two curves indicates that a small additional increment of the depth will generate a much higher strain in the bumper area than in the tail light area. For this reason, the bumper area is considered to be more critical, even though the maximum or final strains for the completed stamping are identical in both areas. Examination of the untrimmed part revealed the reason for this difference in strain history. (14,28,33) Locking beads \* located opposite the tail-light area restricted the material moving in from the flange,

causing large strains to appear at a shallow stamping depth over the punch area. Around the bumper area, however, there were no locking beads; metal freely moving in from the flange reduced the amount of stretching required of the metal in the punch area. However, the sharp point configuration at the bumper area caused the metal to 'lock' between the punch and die just before the panel was completed; all deformation was now confined to a very small area. Consequently, at the end of the stroke, the amount of straining in the bumper area was very high for a small increase in stamping depth.

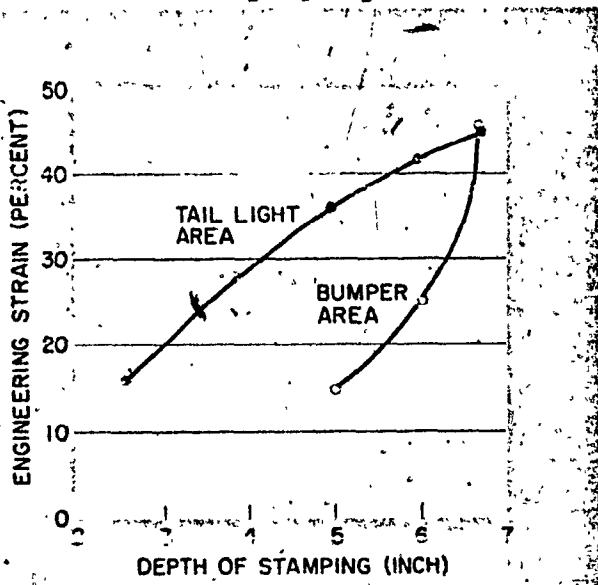


Figure 3.4 Strain histories for the tail-light and bumper areas of the automotive quarter-panel. (From Ref. 14, 28, 33).

- \* Locking beads are mating ridges and grooves in flange sections of dies which restrain movement of the sheet as the part forms.

Wrinkles observed in a finished stamping are often located in a position far removed from their point of origin. Examination of the sequence of progressive stampings are also useful in observing the movement of wrinkles and identifying the conditions causing them.

(28)

### 3.5 FORMING LIMIT DIAGRAM (FLD)

#### 3.5.1 CRITICAL STRAIN LEVEL CURVE (KEELER-GOODWIN CURVE)

Until recently, no analytical technique was available for the study of failure in complex sheet metal stamping.

The Forming Limit Diagram (FLD), as postulated by Keeler (9,14,28,33,36) and further developed by Goodwin, (12)

plays an important role in the measurement of the limit strains achievable in sheet-metal deformation and as a diagnostic aid to sheet-metal forming problems and metal specification. From laboratory deep-drawing and stretching experiments and production stampings, an empirical failure criterion can be established which is based on the measurement of the major and minor principal surface strains of the deformed grid-circle(s) at some critical 'failure' point on the stamping. The empirical failure criterion is a critical combination of the highest principal strain and the secondary principal strain in the surface of the metal sheet. Ignoring the through-thickness strain, the surface

strains can be resolved into a maximum (major) and a minimum (minor) surface strains and these are termed  $e_1$  and  $e_2$  respectively. The very important point is that, at failure, for any value of  $e_1$ , there is a unique value of  $e_2$ . (25, 40) Thus a plot of major strains versus minor strains will give a Critical Strain Level Curve, known as the Goodwin-Keeler Curve of the FLD (11, 12, 15, 25, 36, 37, 40) which separates 'permissible' strains from those which would cause necking and fracture (Figures 3.5, 3.7 and 3.8). Subsequently, the peak strain values for a new pressing or deep-drawing may be referred to the diagram and the success of the pressing operation can be predicted if the point falls below the Goodwin-Keeler Curve.

Most industrial stampings fail under biaxial tension in stretching, which obviously produces positive strains in all directions in the surface of the metal sheet. Keeler (9, 14, 28, 33, 36) analyzed and plotted  $e_1$  against  $e_2$ , resulting in a critical strain level curve (Keeler's Curve) in the Forming Limit Diagram (FLD).

Goodwin (12) extended Keeler's analysis to situations where the minor strain is negative, i.e. the strain state is tension-compression, which is the case when deep-drawing predominates over stretching. (2, 33) The formability limit diagram is given in Figure 3.5.

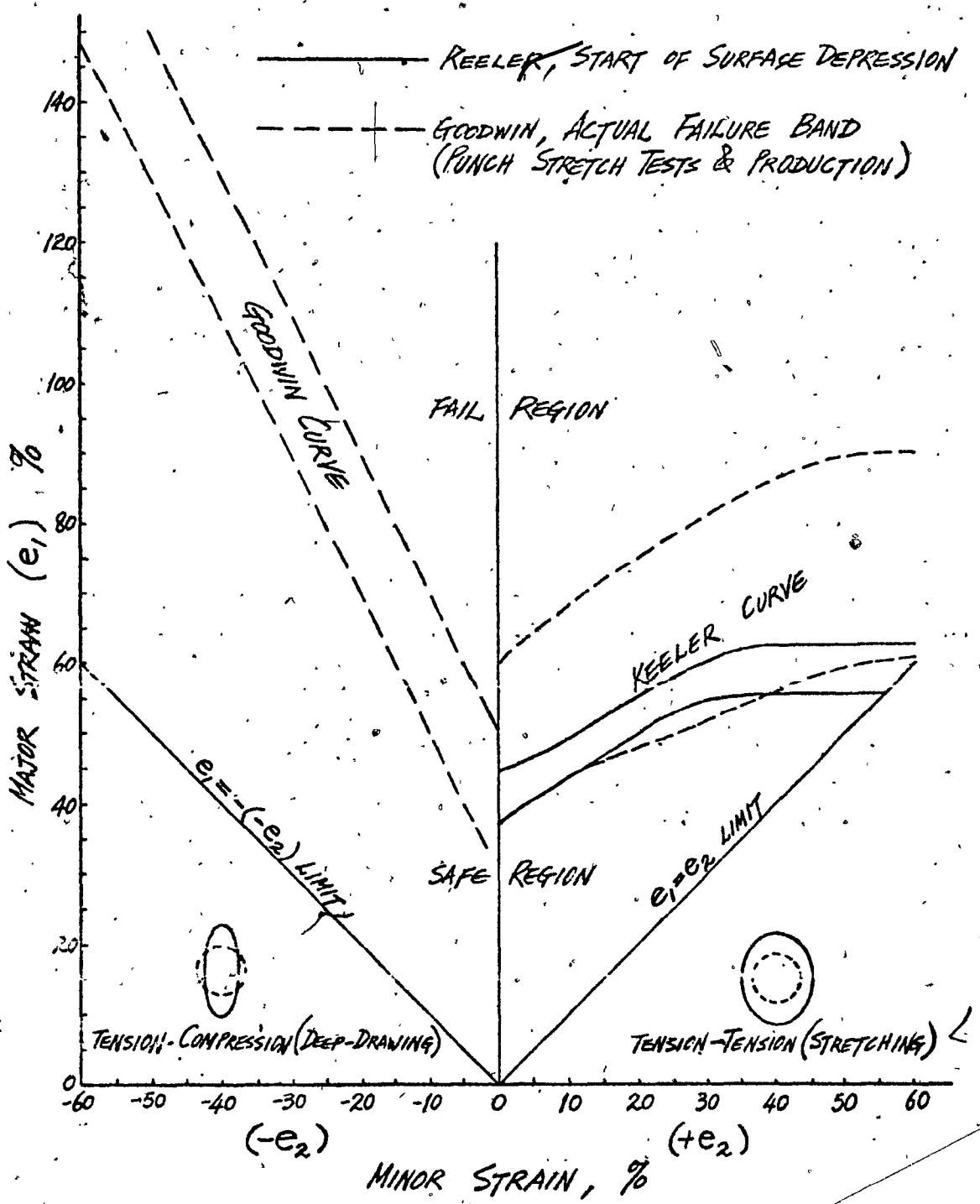


Figure 3.5. Critical strain level curve (Goodwin-Keeler Curve) in the forming limit diagram. (Based on Ref. 2, 12, 33, 38).

Combinations of major and minor strains at any location of a stamping that lie above the curve cannot be achieved without failure, whereas combinations below the curve can be attained without fracture. If the measured strain in any region approaches the curve, the stamping is considered critical. (2)

Because the greater of the two surface strains is, by definition,  $e_1$  and in stretching both strains are positive, then the limits of the FLD are  $e_1 = e_2$ , i.e. the strains produced under balanced biaxial tension. The limits in the deepdrawing region is that for pure radial drawing or pure shear,  $e_1 = -(-e_2)$ .  $e_2 = 0$  represents the limit between stretching under biaxial tensile stresses and deep-drawing under combined tension and compression. (11,25,40)

In the tension-compression regions, very high strains are possible. The magnitude of the major strains can far exceed the strains at fracture in a conventional tensile test. The reason for this - in part - is simply that the metal is compressed normal to the tensile axis, causing a natural elongation in the tensile direction without any tensile force being applied. In this type of deformation, metal can withstand very high strains under compressive stresses without failure. (2,12,33) Failure strains of (148% x - 55%) have been reported by Heyer and Newby (16) for crisper pans which failed at only 8% increase in unit area.

Keeler reported, according to Goodwin,<sup>(12)</sup> that a failure occurred in an instrument panel when the strains were 80%  $\times - 25\%$ .

### 3.5.2 DEFINITION OF THE CRITERION FOR FAILURE FOR THE CRITICAL STRAIN LEVEL

The question of which ellipse is to be measured after the stamping fractures, to provide the most accurate information on the critical strains or determining the precise end point is obviously very important. A number of measures have been tried by many workers<sup>(15, 21, 22, 27, 31,</sup>

36) and in the case of grids containing circles, the following relevant ellipses have been measured:

- (a) An ellipse straddling the fracture.
- (b) The nearest whole unfractured ellipse next to fracture, whether it is above or below the fracture.
- (c) For axisymmetrical stampings, the ellipse in the same position but diametrically opposite the fracture.
- (d) The extrapolated point method.

Definition (a) is not recommended since the ellipse straddling fracture will include material which has passed the point of instability, also it cannot be guaranteed that fracture initiated in that circle and hence strains may be different if it is remote from the area where the fracture began. Also, the problem of measuring

parts of ellipses leads to inaccuracies of measurement.

Woodthorpe and Pearce (15) reported different results of the critical strains measured from the unfractured ellipse above and below the fracture, while being the same essential criterion. However, if due cognizance is given to the chosen circle size and strain gradients existing method (b) gives a reasonably accurate picture of the strain pattern near the failure. Since the material has not failed in the measured zone the results will inevitably be below the fracture strain value of the metal. Nevertheless, if a number of such circles are measured on similar stampings, a picture can be built up of the strain pattern existing. This is the usual preferred measure for routine determinations.

The measurement of the 'equivalent' ellipse in definition (c) gives reproducible 'equivalent' criterion of the major and minor strains. It assumes that the strains on the opposite side of the stamping are identical and this is not always so. This method is of limited application as it can only be used in axisymmetrical situations.

If the fracture strain at zero gauge length (point of fracture) is required, method (d) can be applied. The strains of the major and minor axes of a series of circles

along a line perpendicular to the crack, through the fracture site are plotted as a function of distance (Figure 3.6); it is possible to extrapolate to the maximum strain at the fracture point.

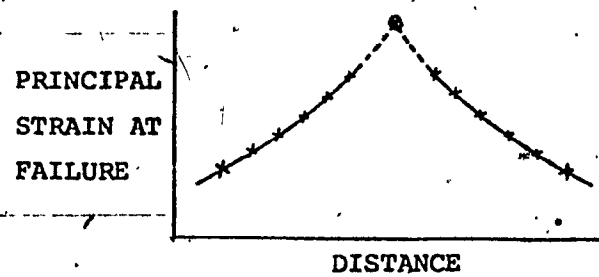


Figure 3.6. Extrapolated point method for determining strain at fracture. (Based on Ref. 21).

The practical value of the FLD-FRACTURE curve is limited because, in practice, localized necking is not allowed for most stampings. Failure is more realistically defined by the onset of localized necking than by the physical separation or tearing of the material. (27,28,31,36) This is perhaps a little too strict because in most ductile metals, a significant strain occurs between the moment of instability and when the metal splits. A wide failure band is created in the FLD, in which the necking strain value is the lower bound and the fracture strain the upper. (25) The criterion (b) for measuring the limiting strain would appear to fall in the above band and one may logically conclude that it be the chosen measure.

### 3.5.3 FACTORS AFFECTING THE CRITICAL STRAIN LEVEL

A reproduction of Keeler's first diagram is shown in Figure 3.7. The causes of scatter in the critical strains can be grouped as follows:

- (a) inaccurate grids.
- (b) lack of definition in the chosen measure of failure (difficulty in defining the limiting uniform strain).
- (c) a wrong choice of the distorted circles to be measured.
- (d) the anisotropy of the sheets.

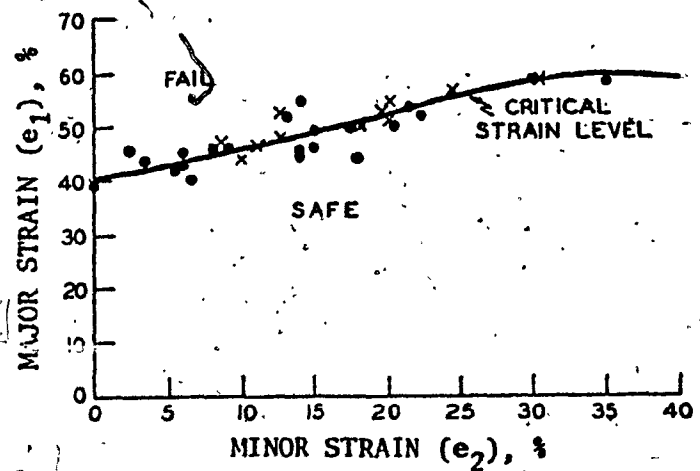


Figure 3.7. Keeler's original FLD represents laboratory biaxial stretching experiments for various annealed materials, punch geometries and lubrication. X represents measurements of production automotive steel stampings.  
(From Ref. 15, 28)

Further work led him to represent his results as a band rather than a line, as shown in Figure 3.8. (14,15,31,38)

Goodwin (12) defined failure strains as those which exist in the necking itself; thus his band has a higher upper limit than Keeler's (start of surface depression) though naturally the lower limit was about the same, refer to Figure 3.5. Thus the level of the band width depends upon the failure criterion.

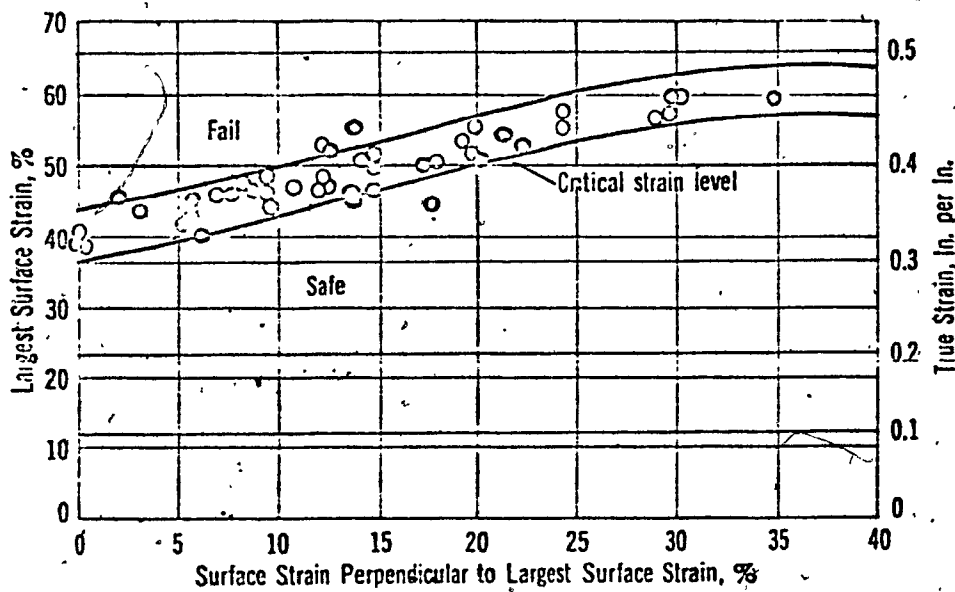


Figure 3.8. Keeler's modified FLD, a wide band separating 'Fail' from 'Safe'. Closed circles indicate results of biaxial stretching experiments for various annealed materials, punch geometries and lubrication. Points indicated by open circles are derived from measurements of automobile steel stampings. (From Ref. 2, 14, 15, 33, 36).

Work by members of the American Deep Drawing Research Group has shown a band with a width of 6-8 percent strain to be a more realistic critical strain curve than a single line. (12,13,33,36)

Keeler (14, 28, 33, 36, 38) reported that the band of the Keeler-Goodwin Curve in the forming limit diagram (Figure 3.9) is applicable for a variety of materials, especially low-carbon steels. It is empirically derived by different laboratory and production stampings formed by punches of different shapes and different lubricants. Specimens are also made from different materials; such as copper, brass, aluminum and steel.

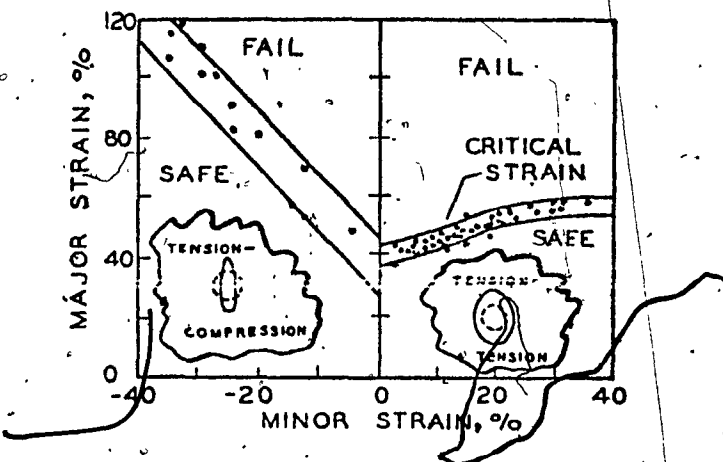


Figure 3.9. The forming limit diagram. (From Ref. 38)

Pearce and Ganguli (11, 25) reported that the different laboratory experimental methods could result in slight variations on the shape and level of the limit strains curve of the forming limit diagram. Figure 3.10 shows some results for commercial-purity aluminum. The open circles represent limit strains obtained for combinations of stretching and some drawing, while the crosses are obtained for stretching only with different lubrication.

systems. The closed circles are hydraulic bulging results using various elliptical dies. It could well be that the critical strain level curve without friction (hydraulic bulging) and that with friction (press-forming) represent the lower and upper bounds of the critical strain level for industrial forming operations under similar conditions.

(11) However, in Pearce's laboratory determination of the FLD for steels, it was found that points obtained by different techniques fell on a common curve,

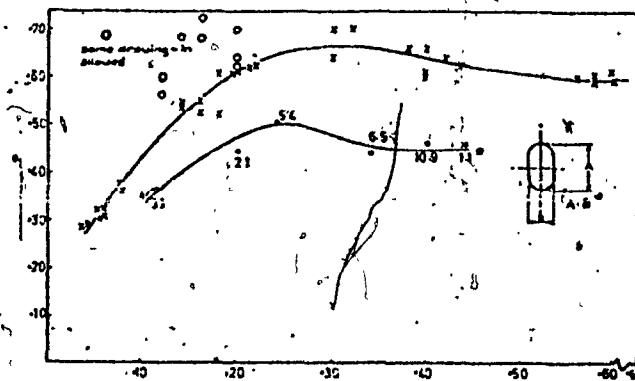


Figure 3.10. Forming limit diagram for commercial-purity Aluminum ( $\sim 99.5\%$  Al) determined by punch-stretching (upper curve) and by hydraulic bulging (lower curve) (From Ref. 11, 25)

and so it must be assumed that the aluminum used is more sensitive to process variables than was the steel used in his earlier work.

In the investigation of the forming limits of aluminum-magnesium alloy sheet in biaxial tension, Pearce and Ganguli (11) reported that the level of the forming limit diagram falls and the curve flattens with increasing magnesium content up to 5.1% (Figure 3.11).

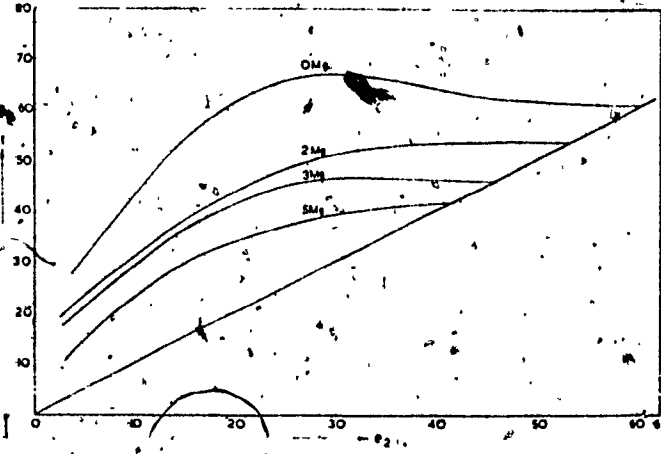


Figure 3.11 Forming limit diagram for aluminum-magnesium alloy sheets. 0 Mg = ~ 99.5% Al, 2 Mg = 2.1% Mg, 3 Mg = 3.7% Mg, 5 Mg = 5.1% Mg. (From Ref. 11, 25).

#### 3.5.4 USE OF THE FORMING LIMIT DIAGRAM (FLD)

Severity rating limits are established by dividing the area under the limiting strain curve into clearly defined zones. (9,22) The curve presented in Figure 3.12 is the one in current (November 1972) use within the Austin-Morris body plant, British Leyland Motor Corporation, Cowley, Oxford, England. (22) The major and minor strain

combination observed at a critical area is plotted at the appropriate spot on the FLD to determine the relative severity of that particular pressing. If a pressing falls consistently into Zone B and C, then consideration might be given to using a lower grade of sheet. Conversely, if a pressing is categorized in Zone A and if the scrap costs become high, then there may be justification for using a higher grade of sheet. This procedure ensures that the optimum grade of steel is utilized and evaluates the forming severity of a particular design.

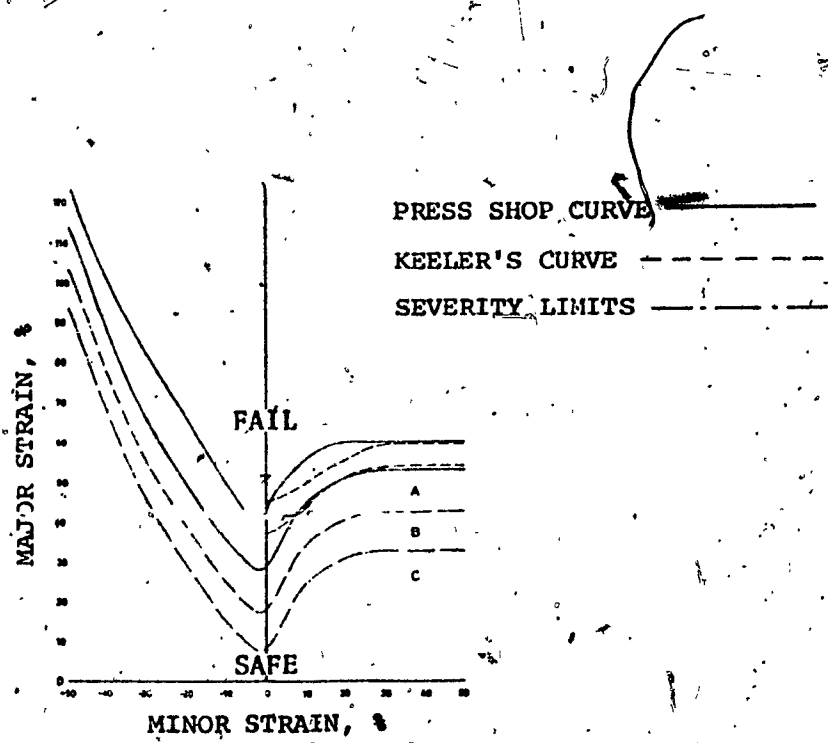


Figure 3.12. Press shop forming limit diagram for steel sheet. (From Ref. 22)

A similar concept that was developed by Palmer (37) for predicting reliability in forming is to plot the Relative Safety Factor (RSF) at any particular location in the stretched or deep-drawn part. For this purpose, the strain values measured from the ellipse of the location is marked on the FLD as point A in Figure 3.13. A line is drawn from the origin through this point to intersect the curve at C. The ratio of the distance of the point from the critical strain curve to the distance from the origin to the point of intersection, gives the RSF for that particular point. Keeler (38) disagreed with Palmer's proposed RSF construction and favoured the value of permissible strain remaining (AB) to be the most meaningful measure of a forming safety factor, see Figure 3.13, since the important item required by tool and die men is the amount of allowable strain in the principal direction remaining between the current strain state in the stamping and the critical strain. Apparently, Keeler has neglected the idea of strain path. Palmer's RSF for any particular point is a measurement of its progression towards failure assuming a constant ratio  $e_1/e_2$  throughout the deformation. However, in actual stampings, variations in the route occur.

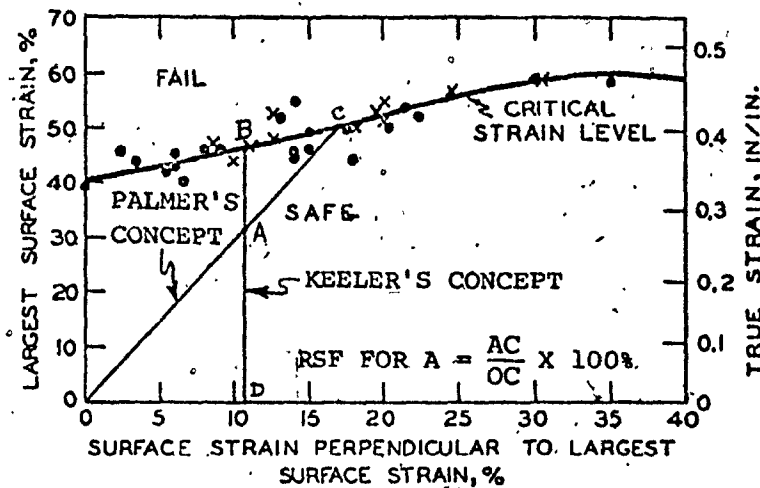


Figure 3.13. Concepts of the Relative Safety Factor (RSF) of a stamping in the forming limit diagram. (Based on Ref. 37, 38)

An interesting feature of the Keeler Curve (Figure 3.5) is that the critical strain level slopes upward; the critical major strain increases with increasing minor strain. From this, it would seem that control of metal flow perpendicular to the maximum strain direction could increase the maximum allowable strain before failure. (14,36)

The following example demonstrates the advantage of evaluating formability by means of the forming limit diagram rather than the measurement of percentage increase in area which was historical press-shop practice. (12,28) A

Stamping with 95% increase in unit area can be formed successfully, whereas a stamping with 65% increase in unit area splits regularly. Relating the strains as measured to the critical strain level curve in the LFD, it becomes apparent why the one with the greatest increase in unit area causes no trouble while the other did. The measured strains for the first stamping were 50% x 30% which falls below the formability limit (Figure 3.7.). The strains in the second stamping were 50% x 10% which lies above the formability limit.

Changing the strain state of a stamping can eliminate failure. (25,33) As shown in Figure 3.14, increase in the minor strain moves the strain state from the failure side to the safe side of the critical strain level curve, avoiding consistent failure. Before the time of the Keeler-Goodwin Curve, the die engineers normally reworked the dies to allow more metal to pull in from the flange parallel to the tear to correct the failure. However, by restricting the flow of metal in from the flange and creating a greater minor strain in this case, failure of the part was avoided.

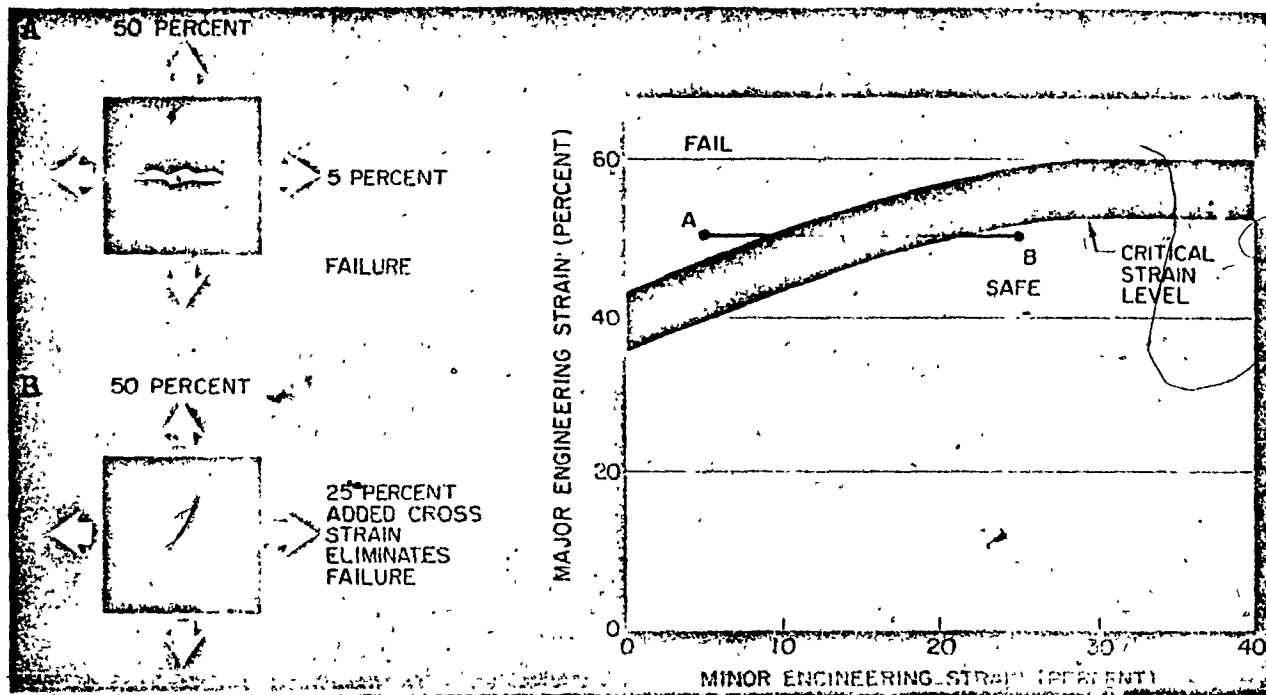


Figure 3.14: Change of the strain state converting failure into a successful stamping.  
(From Ref. 25, 33)

The critical strain level curve also suggests that the highest maximum strain location may not be the failure site. Such a case is observed in a front bumper, as shown in Figure 3.15.

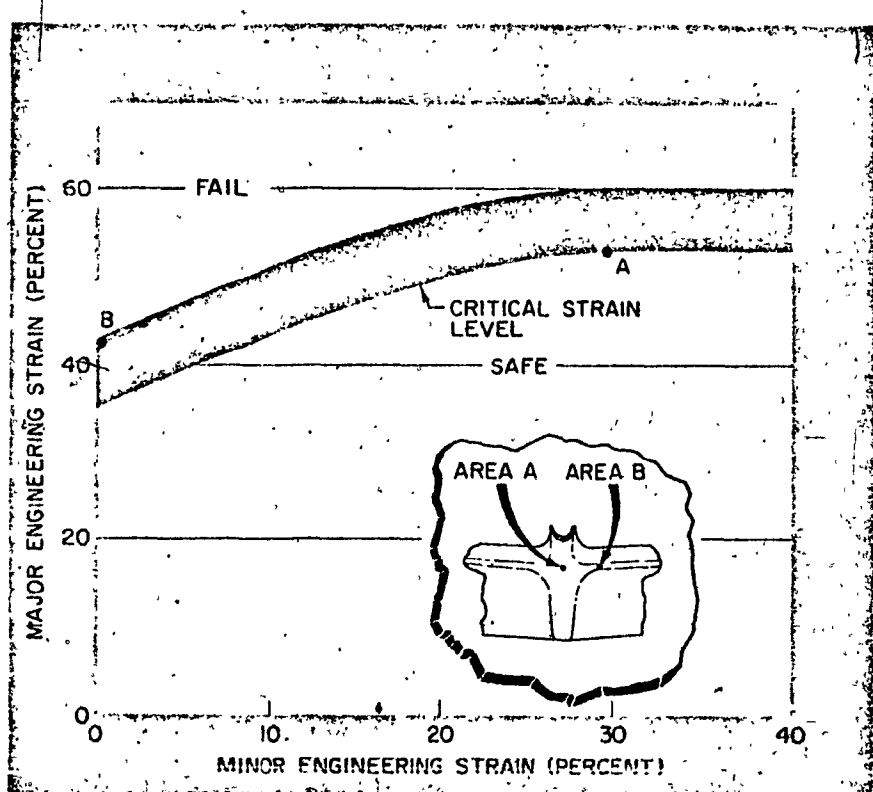


Figure 3.15. Maximum strain may not coincide with the failure site in a formed part. (From Ref. 33)

One limitation of the Keeler-Goodwin Curve is that it cannot be applied to stampings in which the strain in a given region is reversed, from compression to tension during forming. The effect of different strain histories during the course of stamping can raise the limit strains above the critical strain level curve (Figure 3.16). (25) The initial tension + compression can be thought of as thickening up (or at any rate not significantly thinning) the metal before the imposition of biaxial tension, while

in the simple case thinning in tension occurs immediately.

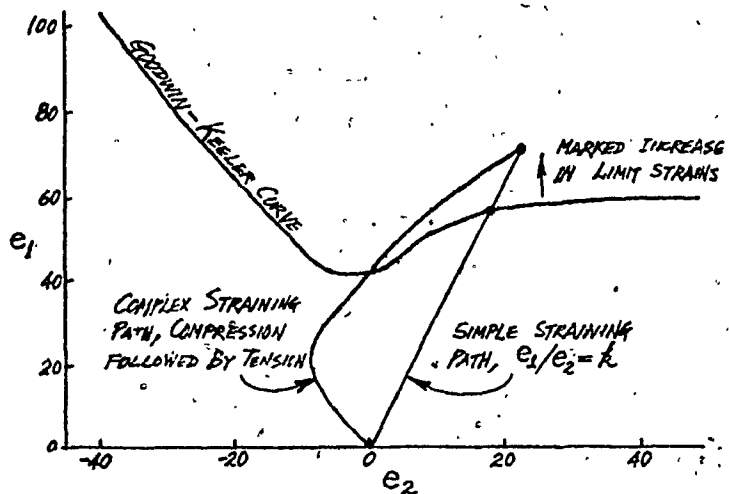


Figure 3.16 Limitation in applying the Keeler-Goodwin Curve. (From Ref. 25)

However, the use of the grid analysis system and the FLD is a valuable aid for evaluating sheet metal formability. The FLD can be used to specify the properties for stampings. (14) A trial blank of the sheet-metal is gridded and formed, if the peak strains measured are just below the critical strain level curve, the mechanical properties of the trial blank are considered to be the minimum property specifications of the material. These properties, in turn, indicate the steel grade and quality to be used.

## CHAPTER 4

### STANDARD MECHANICAL PROPERTIES AFFECTING STRETCHABILITY AND DRAWABILITY

#### 4.1 GENERAL

Of the mechanical properties which can be evaluated by standard tension tests, the only two which strongly influence the formability of sheet-metal are the work-hardening coefficient and the anisotropy coefficient. (13,33,36) Mechanical properties such as yield stress, ultimate tensile strength, total elongation and hardness have either an unknown or an indirect relationship to stretching and drawing.

The work-hardening exponent ( $n$ ) influences the ability of the material to be predominantly stretched. The anisotropy coefficient ( $r$ ) strongly controls the ability of a material to be predominantly deep-drawn into a flat-bottomed cup. A part, judged to be a combination of stretching and drawing, correlates with both  $n$  and  $r$  values. (2,6,14,26,28)

#### 4.2 THE WORK-HARDENING EXPONENT ( $n$ )

A fundamental property associated with ductility is the work-hardening capacity of a metal. This property can be described as the ability of a metal to sustain a greater load while its cross-sectional area is being reduced. Conventional sheet-forming would not be possible for a non-work-hardening metal.

because instability, necking and fracture would occur at the point at which the punch first touched the sheet, for without work-hardening it would not have the ability to strengthen up resisting deformation, and pass the forming load on to a less strained element of the pressing. (19,34)

The amount of work-hardening can be observed by plotting the traditional engineering stress-strain curve obtained from a uniaxial tension test. Theoretical stress-strain curves for materials with high and low n values are shown in Figure 4.1. The material with the higher n value is characterized by a steeper stress-strain curve. This means a greater separation between the ultimate tensile stress and the yield stress. The uniform elongation - the strain value at maximum load - is also larger for increased n values. The engineering stress-strain curve is not a realistic way of describing the material behaviour especially immediately after necking begins. Once necking begins, geometrical softening (reduction in load due to reduced cross-section) is greater than the work hardening of the material.

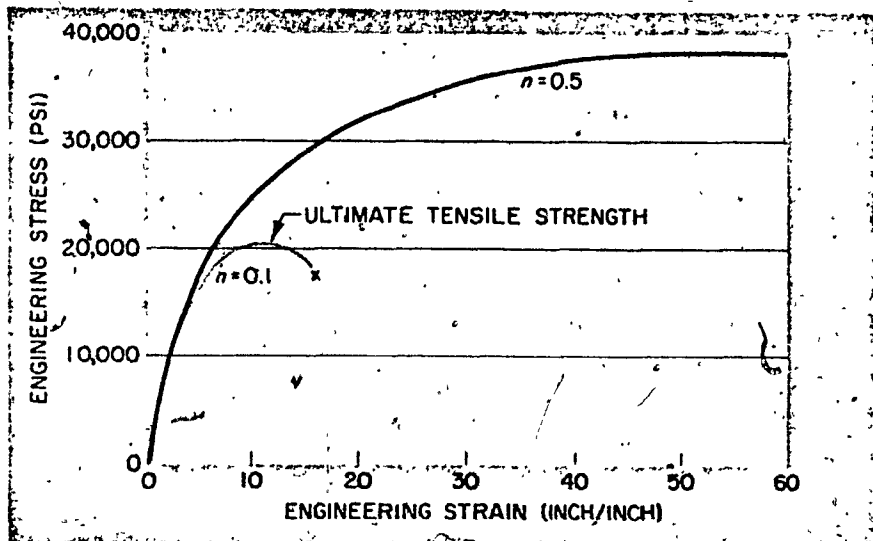


Figure 4.1. Engineering stress-strain curves. (From Ref. 33)

The equivalent true stress ( $\sigma$ ) and true strain ( $\epsilon$ ) curves for the two  $n$  values plotted in Figure 4.1 are given in Figure 4.2. The stress-strain curves for many metals, especially low-carbon steel, can be approximated by the power law equation which is applicable from above the yield strain to somewhat beyond the strain at maximum load.

$$\sigma = K \epsilon^n$$

where  $K$  is a constant for the material. The work-hardening coefficient ( $n$ ) is defined as the exponent of the stress-strain relationship. The higher the  $n$  value, the more the material work hardens (2,7,13,14,19,20,26,33,34) and the higher is the tensile stress/yield stress ratio. Moreover, the magnitude of  $n$  is

equal to the uniform elongation, the true strain at the onset of necking (at which the load reaches a maximum). A more nearly uniform strain distribution in stamping is obtained from material having a higher uniform elongation; (32,33) thus the higher the  $n$  value, the greater the resistance to necking. The use of uniform elongation as a criterion of formability is preferred to the use of  $n$  because it is directly related to the limiting strains at tensile instability, whereas the work-hardening coefficient is derived for low strains which may not be applicable for the whole stress-strain curve. (7)

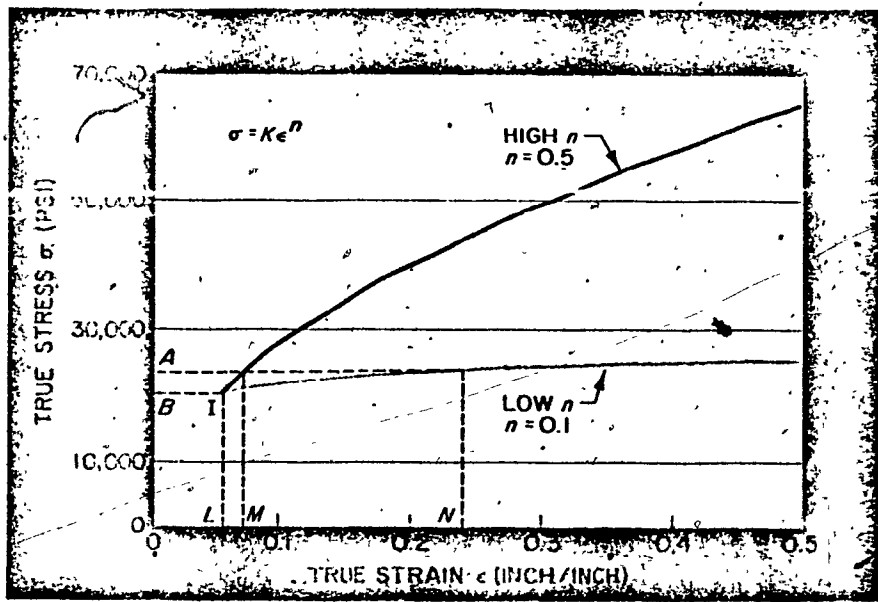


Figure 4.2. True stress-strain curve. (From Ref. 33)

Some typical  $n$  values for room temperature are given here to indicate the range of expected values: (33)

Aluminum                    0.20

Low Carbon Steel        0.25

Copper                    0.30

Brass	0.40
Stainless Steel	0.50

To obtain a true evaluation of  $n$ , tests should be performed in directions 0, 45 and 90 degrees from the rolling direction.

#### 4.2.1 METHODS FOR EVALUATING THE $n$ VALUE

##### (a) Logarithmic plotting of the true stress-strain curve

There are several ways for obtaining the  $n$  value of a material. (3,19,26,33,34) The stress strain relationship  $\sigma = K\epsilon^n$  may be rewritten as  $\log \sigma = \log K + n \log \epsilon$ . Thus when both  $\sigma$  and  $\epsilon$  are plotted on logarithmic scales, the stress strain curve should be a straight line having the slope  $n$ . (26,29,30,33)

The value of  $K$  is the stress intercept of the line at a strain value of 1.0 (Figure 4.3).

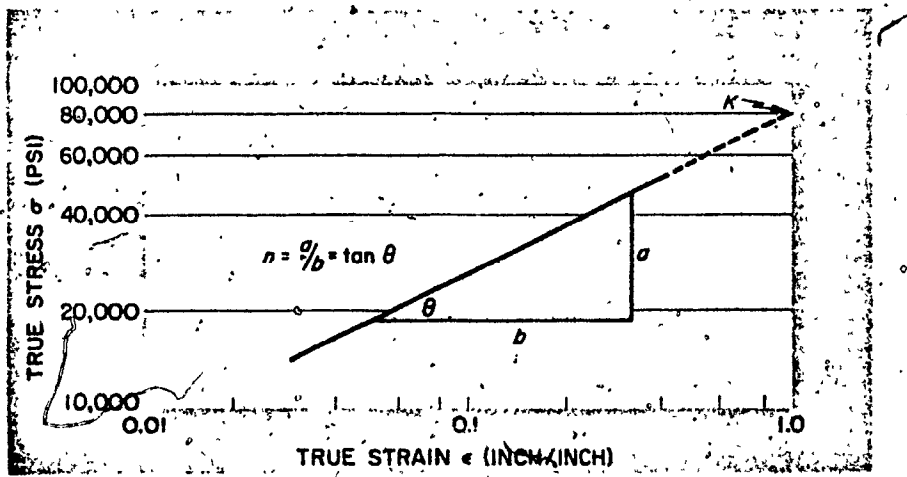


Figure 4.3. Calculation of  $n$  value from true stress-strain curve. (From Ref. 33)

For most low carbon steels and many of the non-ferrous metals commonly used in the forming industry, the  $\log \sigma - \log \epsilon$  plots are approximately straight and a value of  $n$  can be determined. The  $\log \sigma - \log \epsilon$  plot may have two straight segments and hence two  $n$  and  $K$  values; this occurs for some stainless steels. If, for some of the less-common metals, the logarithmic stress-strain plot is curved,  $n$  varies with strain being the slope of the curve at each point. Under these conditions, the use of  $n$  is no longer valuable and the uniform elongation, becomes the appropriate parameter to determine.

While this method has the advantage that it indicates visually whether the empirical equation is applicable, it is too time-consuming to be used for routine testing.

(b) NELSON-WINLOCK PROCEDURE (LOAD MEASUREMENT METHOD)

The Nelson-Winlock procedure assumes that the log stress-log strain equation plots as a straight line. (6,20,26,33)

Therefore any two points are sufficient to define the curve and permit calculation of the  $n$  value. Two convenient strain values are chosen and the load at each point is recorded. One point, the easiest to measure, is the maximum load ( $P_u$ ). The other load value can be obtained at any strain value that avoids the initial portion of the curve containing yield point elongation and other variations.

For convenience, the load is recorded at 10 percent elongation ( $P_{10}$ ). Any crosshead speed can be used, although 0.2 ipm is convenient. It is important that the strain rate be kept constant between  $P_{10}$  and  $P_u$ .

The ratio  $P_u/P_{10}$  is calculated and the  $n$  value obtained from a graph, see Figure 4.4. The precision of the Nelson-Winlock method is currently limited to about  $n = 0.02$ , according to work done by the American Deep Drawing Research Group.

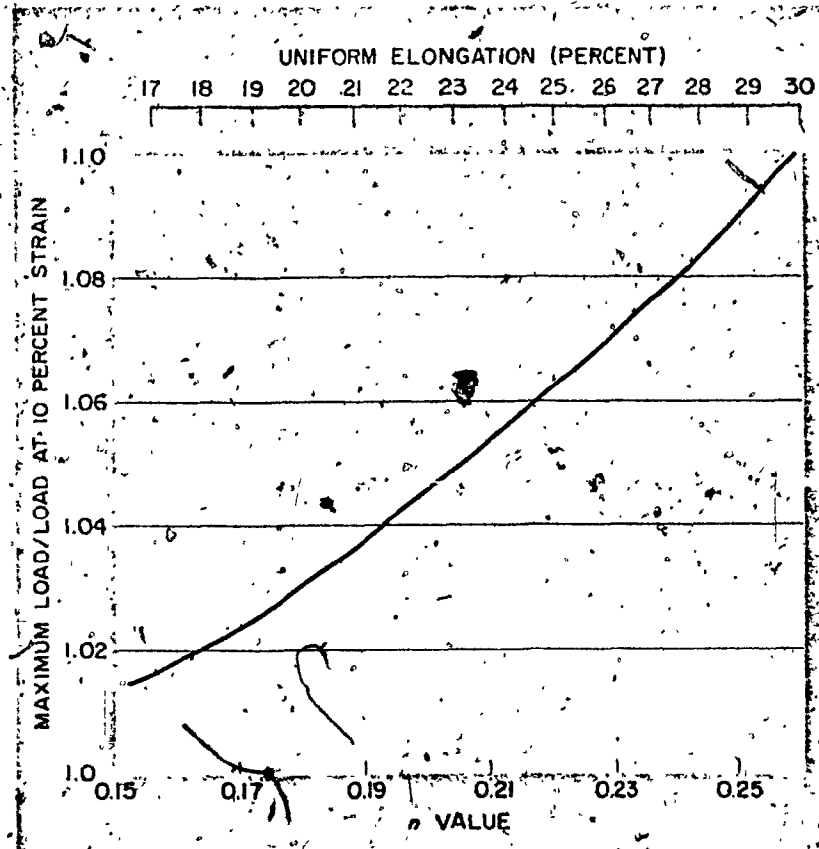


Figure 4.4 Nelson-Winlock relationship between  $n$  and the ratio of maximum load to load at 10 percent strain. (From Ref. 6, 33).

(c) STEPPED SPECIMEN TECHNIQUE

The stepped tension test specimen as shown in Figure 4.5 was developed by Heyer and Newby of the Armco Steel Corporation, U.S.A. (3) It is designed to give conventional tensile properties from data based on the narrowest section since fracture normally occurs in cross-section  $W_0$ . This specimen develops uniform tensile strains in the wider sections of the order of 10 percent in  $W_2$  and 20 percent in  $W_1$  when testing typical low carbon steel sheets. The  $n$  value is calculated from the length strains in these sections, which in effect establish two points on the flow curve, (3,30). It is found that  $n$  obtained in this manner is slightly higher than  $n$  for a standard tension specimen. An explanation for this is based on the fact that the strain rate of the widest section ( $W_2$ ) is lower than the strain rate of the narrow middle section ( $W_1$ ). This results in a relatively lower stress at the lower strain, thus giving a higher slope and numerical value of  $n$ .

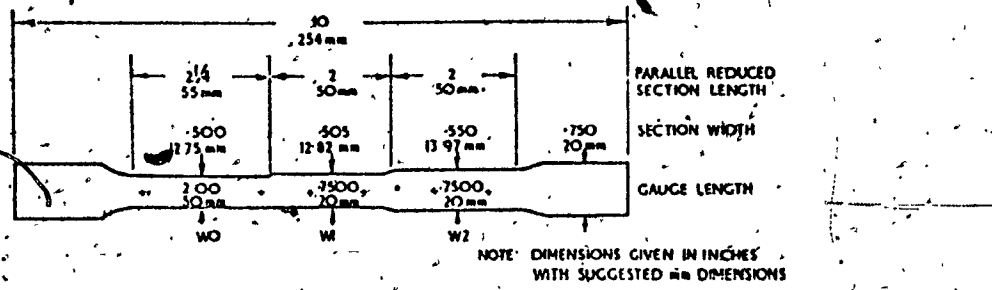


Figure 4.5. Armco three-step tension test specimen.  
(From Ref. 3, 30)

(d) MEASUREMENT OF MAXIMUM UNIFORM ELONGATION BY TWO-STEPPED AND CIRCLE-ARC TENSION SPECIMENS TECHNIQUES

The strain,  $\epsilon_u$ , corresponding to maximum uniform elongation in the tensile test is numerically equal to the strain hardening index in most annealed materials. There are, however, a number of experimental difficulties inherent in determining  $\epsilon_u$ . The strain  $\epsilon_u$  could be derived from the elongation at maximum load as indicated by a load-gauge length extension diagram, but frequently the load is very nearly constant over a large range of extension and it is difficult to determine exactly the point of maximum load. An alternative method is to measure the extension over a gauge length some distance from the neck in a specimen which has been pulled to failure. This may introduce errors as the strain frequently varies continuously along the specimen and the measured value of  $n$  would depend on the choice of area for the gauge length. With either procedure, pre-straining of the material will influence  $\epsilon_u$  and there will be scatter in the test results due to local strain variations.

(26)

By making one portion of the gauge section slightly smaller in width than the remainder of the section in a special two-step tensile specimen, failure will almost always occur in the reduced-width section. When the difference in width of the parallel sections of such a two-step specimen is small,

the elongation of the wider section approaches the uniform elongation, or the elongation at maximum load of the standard tension test. The specimen shown in Figure 4.6, developed by SOLLAC (Societe Lorraine de Laminage Continu) of France, with a difference in width of only 2 percent is of this type.

(3,26) A relatively small correlation is needed to convert the strain in the wider section to a uniform elongation strain, or to the corresponding exponent n.

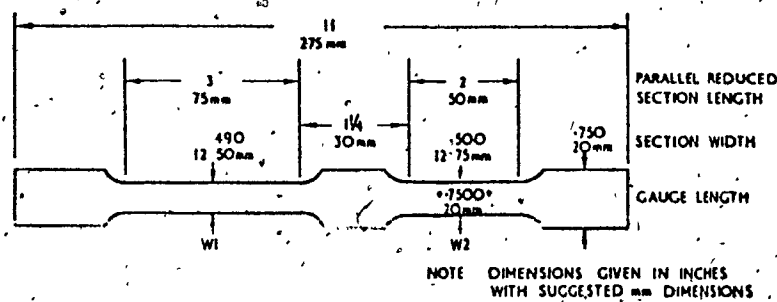


Figure 4.6. SOLLAC two-step tension test specimen  
(From Ref. 3)

Rather than using a complete two-step specimen, Heyer and Newby (3) modified the slightly reduced section in the form of a circle arc. Figure 4.7 shows this circle-arc specimen. The elongation in the gauge marked section is the work-hardening index in the test. The circle-arc reduced section is adopted for ease in machining and to permit a longer parallel section, free from shoulder or grip effects. Pins are used in the specimen ends for alignment in the grips. The major advantage of the techniques of the three-stepped, two-

stepped and circle-arc tensile specimens is that no load or elongation measurements are required during testing; the specimen need only be broken. The desired value is read directly from the broken specimen. This greatly simplifies testing at high strain rates and at other than ambient temperatures. (3,26,33)

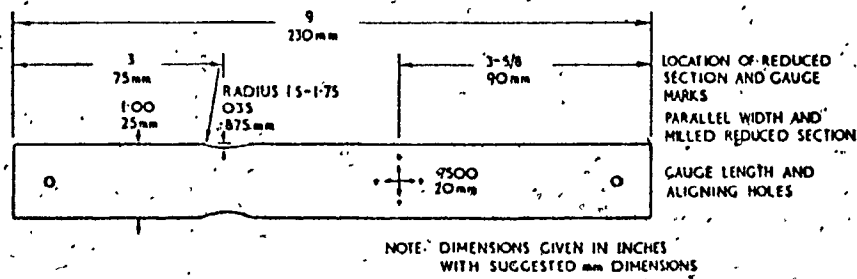


Figure 4.7. Armco Circle-arc tension test specimen.  
(From Ref. 3, 33)

#### 4.2.2 FACTORS INFLUENCING WORK-HARDENING EXPONENT

The higher the tensile-yield stress ratio of an alloy, the higher the work-hardening capacity of the metal, and the better it is for stamping. A high value of this ratio appears as a rising load/elongation curve such as A in Figure 4.8. When such an alloy is deformed locally, that region becomes sufficiently stronger and resistant to further deformation before instability, necking and fracture occur, that the stress in adjoining regions are raised above the yield stress and plastic flow proceeds. In a material with

a low rate of work-hardening - low tensile/yield ratio, flat load/elongation curve B in Figure 4.8 - hardening-up and redistribution of the stress can only take place to a very limited degree, and consequently necking and fracture can occur at the point when the punch first touches the metal blank. Figure 4.9 shows the relationship between work-hardening rate and the yield-tensile ratio, and even though there is considerable scatter in the results, it is clear that lower yield-tensile ratios indicate better work-hardening characteristics. (32)

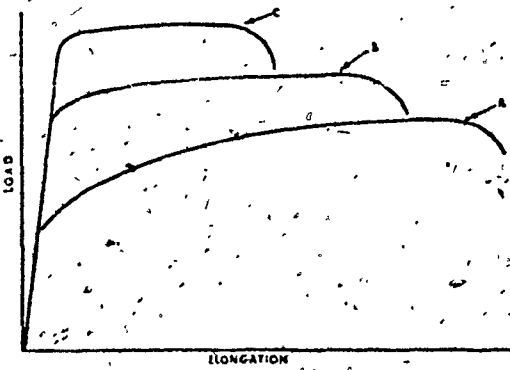


Figure 4.8. Effect of the work-hardening rate of the metal on the shape of the stress-strain curve.  
(From Ref. 32)

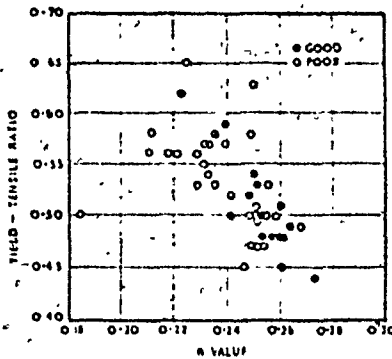


Figure 4.9. Relationship between the yield-tensile ratio and the work-hardening coefficient. The results are obtained when metal for a car fender pressing is assessed. (From Ref. 32)

As with most properties, the values are influenced by testing techniques, testing speed, temperature and direction from which the specimen is removed from the sheet. The  $n$  value will also decrease with aging of rimmed steel and with cold working. (3,33)

#### 4.2.3 EFFECT OF WORK-HARDENING EXPONENT ON STRETCHING

The  $n$  value primarily influences stretchability. (15,20,33) The ability to work-harden locally, when thinning begins, aids in the distribution of strain uniformly over the area being deformed. The most important effect of a high  $n$  value is to improve the uniformity of the strain distribution in the

presence of a stress gradient and this leads to overall higher-strains, since localized straining is postponed. This effect can be shown in Figure 4.2.

Assume for simplicity that two materials have the same stress level ( $B = 20,000\text{psi}$ ) for an initial strain value of  $L=0.05 \text{ inch/inch}$ . Let the stress value at some adjacent location in the stamping be  $A=23,000 \text{ psi}$ . The strain value at this location for the high  $n$  material would be only 0.07 or an increase of 0.02.

The low  $n$  material, however, would strain to a value of 0.24. This increase of 0.19 is ten times that of the high  $n$  material. This would create a highly non-uniform strain distribution - a very undesirable condition. In addition to the high peak strain, a low  $n$  material begins necking at a lower strain value. Necking creates an even greater non-uniformity of the strain distributions.

The effects of  $n$  value on strain distribution can be shown by plotting measured strain values as a function of location on the blank. The example (13) shown in Figure 4.10 is based on the stretch cup tests with drawing-compound lubrication. Figure 4.11 is obtained on the forming of an automotive fender. (33) Both indicate that increased strain hardening extends the zones of high strain over a larger area and

reduces the strain at one specific point. The material with the high  $n$  value gives a more uniform strain distribution, hence there is less chance it will tear during stretching.

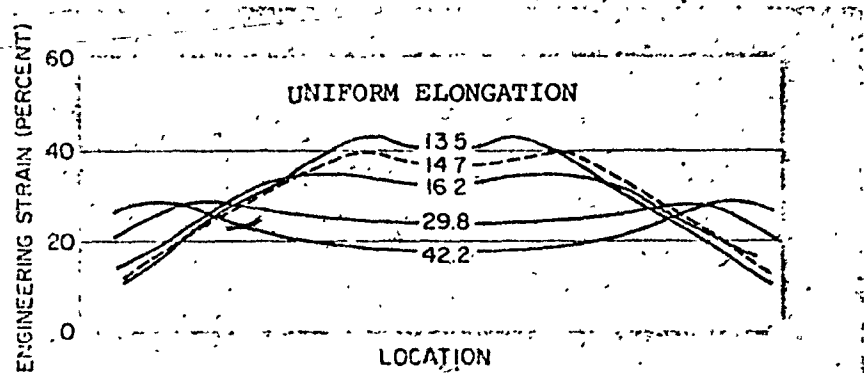


Figure 4.10 Effect of work-hardening capacity on radial strain distribution after stretching to a cup height of 3.1 inches without fracture, with drawing-compound lubrication. (From Ref. 13, 33).

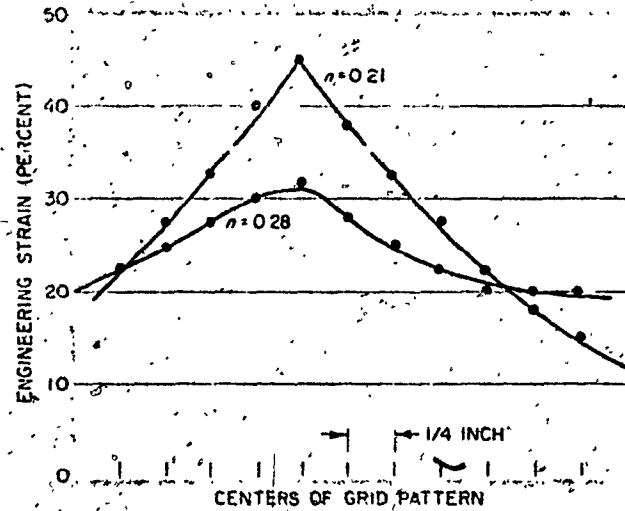


Figure 4.11 Effect of  $n$  value on strain distribution in a formed automotive fender. (From Ref. 33)

Aluminum-killed steel is considered a better quality drawing steel than rimmed steel because it has higher  $n$ -values. Additionally, aluminum-killed steel is stabilized and retains its favourable stretching properties, whereas rimmed steel ages and its properties becomes less favourable with time. In drawing situations aluminum-killed steel generally has higher  $r$  values, which contributes further to better deep drawability. The strain distributions at the critical area of a production automobile license-plate housing formed from these two steels (Figure 4.12) demonstrate the ability of the aluminum-killed steel sheet to distribute the strain more uniformly than rimmed steel.

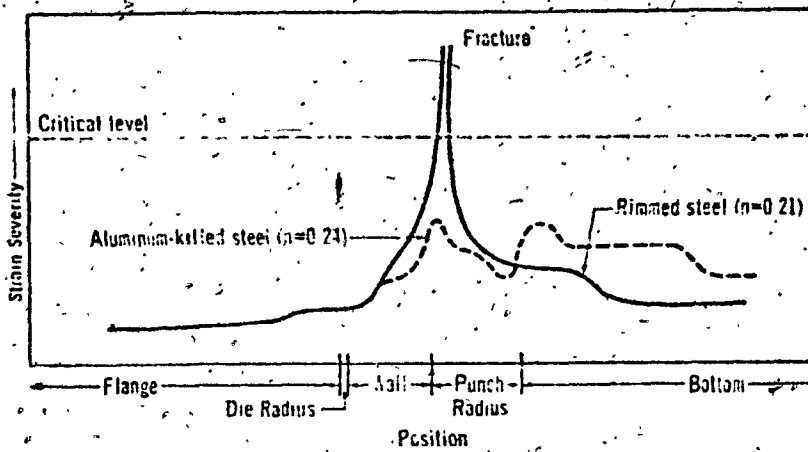


Figure 4.12. Distribution of principal strain of a production automobile license-plate housing formed by two steels. (From Ref. 9).

The influence of lower tensile-yield stress ratio and  $n$  value of a rimmed steel compared with those of an aluminum-killed steel is observed in the strain histories in an automotive quarter panel (33) (Figure 4.13). The peak strain value observed in the stamping made of rimmed steel is considerably higher than that of the stamping made of aluminum-killed steel.

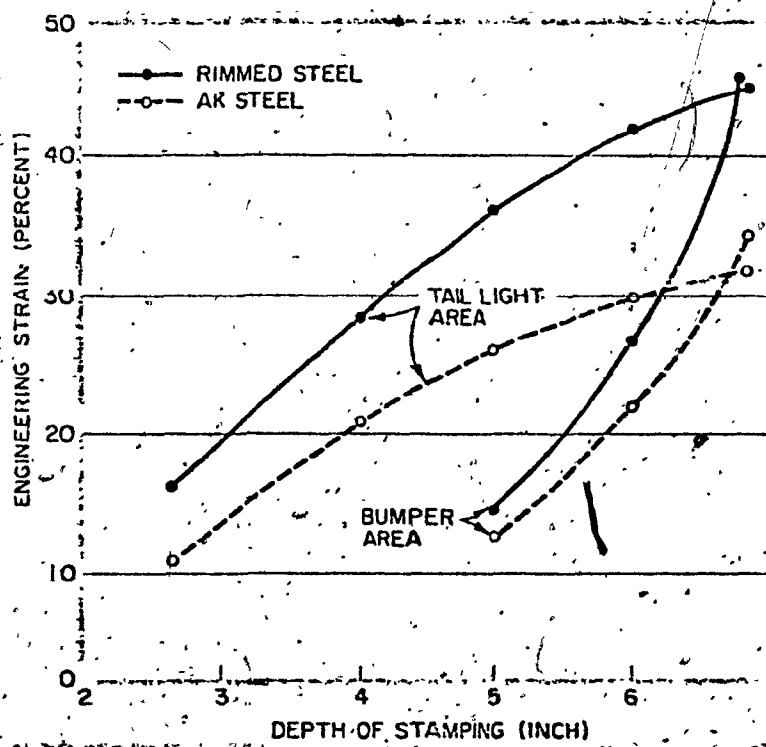


Figure 4.13 Principal strain histories with stamping depth for two areas of biaxial stretch in a production automotive quarter panel using two kinds of steel. Last value is for part completed. (From Ref. 33)

The effect of the work-hardening exponent and the tensile-yield stress ratio on stretchability is shown for a critical area in forming a production automotive fender (28,33) in Figure 4.14. Two rimmed steels with different tensile-yield ratios and n values are compared. Comparison of the properties of the two rimmed steels illustrated showed a tensile-yield stress ratio of 1.35 for A and 1.52 for B. The n values were 0.19 for A and 0.22 for B.

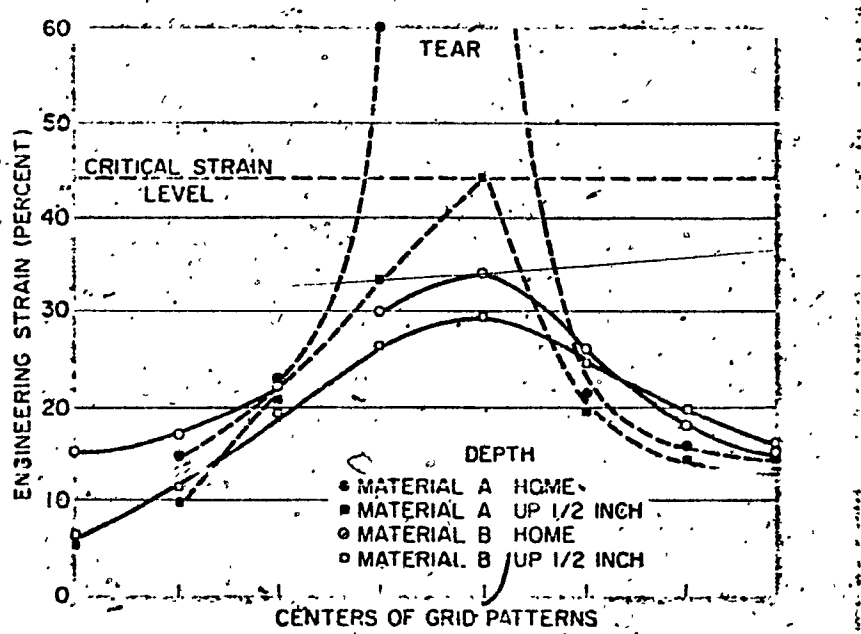


Figure 4.14 The distribution of principal strain of a critical area of biaxial stretch in a production automotive fender. The critical strain level is predicted from the critical strain level curve in FLD. (From Ref. 28, 33).

Keeler (9,28,33) and Goodwin (12) had conducted laboratory and production investigations to determine the influence of material properties on formability. The distribution of strain in three materials (brass, steel, aluminum) stretched over a 4-inch diameter hemispherical punch is plotted in Figure 4.15. Comparison reveals that approximately the same maximum strain level was reached in all three materials because of same geometry. However, the depth is proportional to the area under the curve. Greater depth before failure was therefore achieved in the material having the most nearly uniform strain distribution, which is the material with the highest "n" - type properties. High "n"-type properties are high tensile/yield stress ratio, high uniform elongation, and an overall steep stress-strain curve.

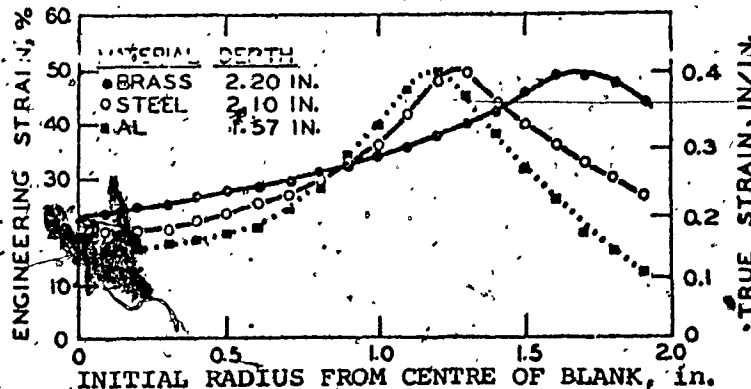


Figure 4.15 Distribution of principal strain at maximum (failure) depth for lubricated materials securely clamped and stretched over a 4-in dia. hemispherical punch.  
(From Ref. 28, 33)

Woodthorpe and Pearce (15) investigated the effect of

$n$  value upon the FLD by performing laboratory stretching

cup tests on aluminum-killed steel sheets. The results

are shown in Figure 4.16 and all the values plotted are

from 45 degrees fractures. It will be seen that the

level of the curve falls with increasing cold work,

which affects  $n$  markedly without much change in  $r$ .

The FLD shows a definite alteration in shape and level.

As the degree of cold work increases, the peak in the

curve becomes lower, eventually disappearing to give a

gradual increase in  $e_1$  and  $e_2$  from the plane strain to

the balanced biaxial end of the diagram. Accompanying

this shape change is an expected downward displacement

of the curve.

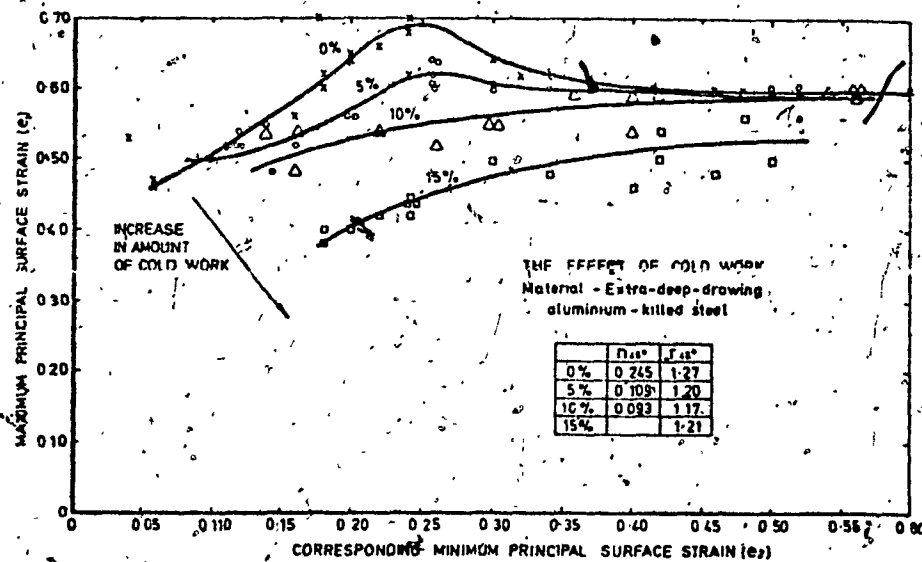


Figure 4.16 Effect of  $n$  upon the shape and position of the FLD. (From Ref. 15, 25)

#### 4.2.4 EFFECT OF WORK-HARDENING EXPONENT ON DEEP-DRAWING

Theoretical and experimental work has shown that the radial drawing limit is little influenced by the strain-hardening capacity of the material. (14, 28, 33)

#### 4.3 PLASTIC ANISOTROPY COEFFICIENT (STRAIN RATIO), $r$

The common assumption that sheet-metal is mechanically isotropic, i.e. the mechanical properties are independent of direction of measurement within the sheet is not well founded considering its method of manufacture. Reduction of metal from an ingot into a sheet, and its subsequent fabrication, create various types of directionality or anisotropy or properties in almost all metals.

The overall shape of the stress-strain curve, and the attendant properties such as yield stress, tensile strength and rate of work hardening, are affected by the presence of preferred crystallographic orientation. The anisotropy of mechanical behaviour has been regarded as undesirable if it leads to earing in deep-drawn cups.

Wrought metal may contain more than half a billion grains or crystals per cubic inch, each with its own identifiable orientation. Since the individual grains are mechanically anisotropic, it is only when crystal orientation is completely random, i.e. all orientations of grains are present on all equal basis, that the

material is isotropic with respect to the associated mechanical properties. However, as a result of this anisotropic behaviour in previous deformation there is a possibility that the grains have certain crystallographic planes or directions aligned with directions of prior working. As a result of the slip systems of many grains being oriented in the same way, different flow strengths are exhibited in different directions and thus deformation is easier and greater in some directions than in others.

This condition of plastic anisotropy (5,32,33) is most apparent as differences between the plasticity properties in the rolling direction and those either in the transverse direction in the plane of the sheet or in the thickness direction. Differences in the rolling and transverse directions are easily measured by means of suitably oriented specimens; however, it is very difficult to determine them in the thickness direction directly. The degree of plastic anisotropy in the thickness properties can be estimated by calculating the strain ratio ( $r$ ), which is defined as the ratio ( $E_w/E_t$ ) of the true width strain ( $E_w$ ) to true thickness strain ( $E_t$ ) as measured in the uniaxial tension test.

(2,10,20) For perfectly isotropic or non-directional sheet, the  $r$  value would be equal to unity; any departure from unity indicates anisotropy. (10,19,20,34) For most steels and other materials, there is a variation of the  $r$  value with direction in the plane of the sheet. A value of  $r$  greater than unity indicates that the strength in the thickness direction is greater than that

in the plane of the sheet and conversely when  $r$  is less.

#### 4.3.1 METHOD FOR DETERMINATION OF THE STRAIN RATIO

The  $r$  value as a function of strain is obtained from a graph of the width strain ( $\epsilon_w$ ) against the thickness strain ( $\epsilon_t$ ) for specimen elongations up to necking in a tensile test.

For most common forming materials, the plot is a straight line and thus the  $r$  value, the slope of the curve, is constant. On the assumption that the plot of  $\epsilon_w$  versus  $\epsilon_t$  is a straight line passing through the origin only one data point at some convenient elongation, such as 15 or 20 percent, is required.

The general test procedures, also suggested by the International Deep-Drawing Research Group,<sup>(6)</sup> is as follows:

(2,5,14,18,19,20,29,30,32,33)

61 Standard ASTM 2-inch gauge length uniaxial tensile specimens, or other specimens with parallel sides and gauge lengths at least four times the specimen width, are cut from the sheet at 0, 45 and 90 degrees to the rolling direction.

- (b) A gauge length ( $l_o$ ), usually 2 inches, is accurately marked on the specimen. The initial width ( $W_o$ ) of the specimen is measured at four points within the gauge length and an average width is obtained.
- (c) Each specimen is elongated at any convenient strain rate to approximately 15 percent which must be below the strain at which necking begins.
- (d) The final gauge length ( $l_f$ ) and gauge width ( $W_f$ ) are measured. This can be suitably done on the specimens shown in Figures 4.5 and 4.7.
- (e) The  $r$  value is obtained by one of the following methods:-

(i) Whereas the definition of  $r$  is:-

$$r = \frac{\epsilon_w}{\epsilon_t} = \frac{\ln e_w}{\ln e_t} = \frac{\ln (W_f/W_o)}{\ln (t_f/t_o)}$$

where  $\epsilon_w$  = true width strain;  $\epsilon_t$  = true thickness strain;

$e_w$  = engineering width strain;  $e_t$  = engineering thickness strain;

$W_o$  = initial width;

$W_f$  = final width;

$t_o$  = initial thickness;

$t_f$  = final thickness.

large errors are possible in measuring the thickness of thin sheets. In addition, the surface roughness of mild steel for pressing may easily correspond to a thickness variation, from place to place on the sample, of  $\pm 0.0005$  inch. The formula can be re-written in terms of the width and length strains of the specimen using the assumption that the volume of the metal remains constant during plastic deformation:

$$r = \frac{\ln (\frac{W_o}{W_f})}{\ln (\frac{l_{ff}}{l_{oo}})}$$

where  $l_o$  = initial length;  $l_f$  = final length.

(ii) In order to save considerable calculation time, a nomograph can be used to obtain a value for  $r$ , as shown in Figure 4.17.

Iafferty, Schmidt and Lawley (17) determined the plastic strain-ratio ( $r$ ) to an accuracy of  $\pm 0.01$  by photo-graphing a grid pattern electrochemically etched on the flat face of the tensile sample at several strainings during a normal tensile test. Changes in grid dimensions as a function of strain are subsequently measured directly on the photographic negatives. Determinations of the  $r$  value for 70/30 brass by this technique appear in Figure 4.18 and show a dependence of  $r$  on strain.

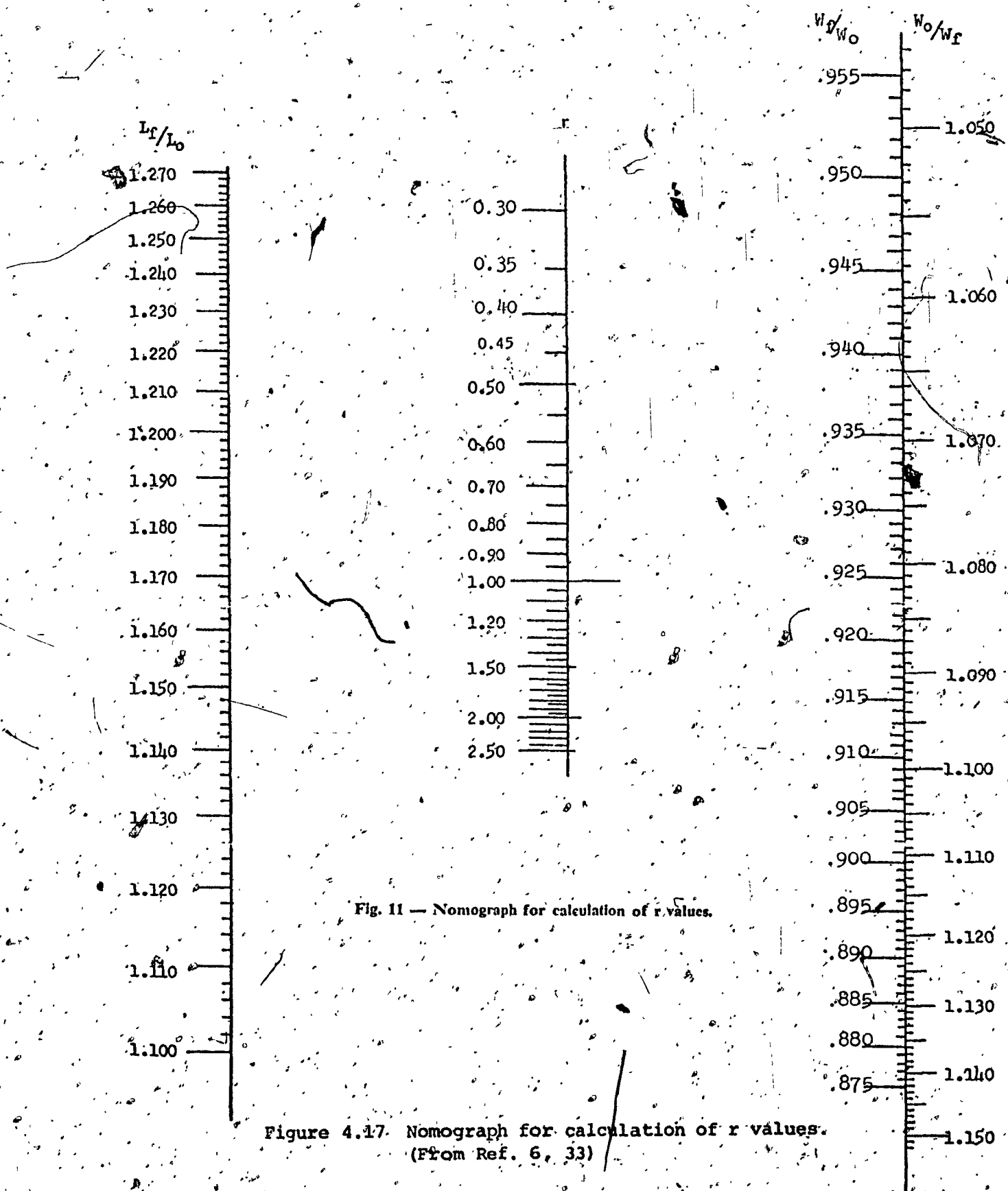


Fig. 11 — Nomograph for calculation of  $r$  values.

Figure 4.17. Nomograph for calculation of  $r$  values.  
(From Ref. 6, 33)

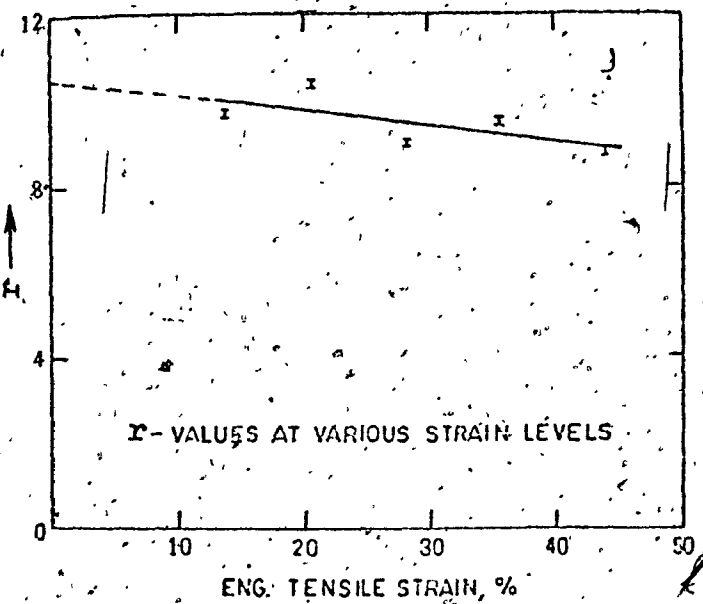


Figure 4.18 Variation of the r-parameter with tensile strain for 70/30 brass. (From Ref. 17).

#### 4.3.2 PLANAR ANISOTROPY COEFFICIENT ( $\Delta r$ )

When  $r$  is not equal to unity but is constant regardless of the direction of the tensile specimen in the plane of the sheet, then the sheet-metal is said to have planar isotropy. For most steels and other materials, however, there is a variation of  $r$  for different directions in the plane of sheet. (5, 10, 33). The variation ( $\Delta r$ ) is called the planar anisotropy and is responsible for earing in deep-drawn cups. The height of the ears being indicative of the magnitude of  $\Delta r$ . As such, planar anisotropy is usually considered objectionable in drawing quality steels.

Planar anisotropy is defined as the difference between ( $r_{45}$ ), the  $r$  value at 45 degrees to the rolling direction and the average value in the rolling ( $r_0$ ) and transverse ( $r_{90}$ ) directions:

$$\Delta r = \frac{r_0 + r_{90} - 2r_{45}}{2}$$

This variation in strain ratio, as shown in Figure 4.19 reflects the degree of planar anisotropy.

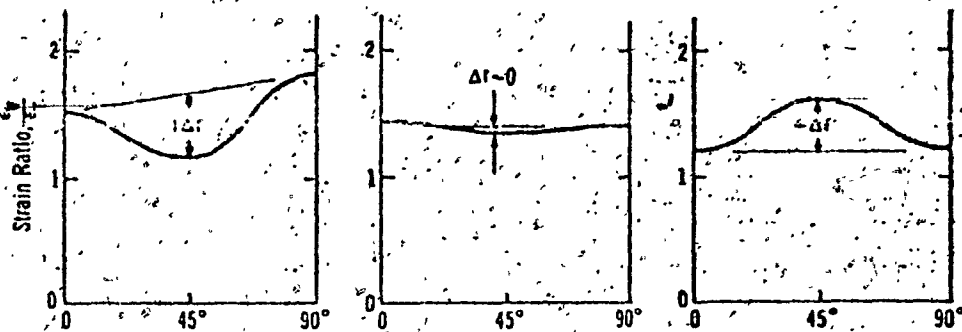


Figure 4.19 The degree of planar anisotropy  
(From Ref. 10)

#### 4.3.3 NORMAL ANISOTROPY COEFFICIENT ( $\bar{r}$ )

The normal anisotropy coefficient ( $\bar{r}$ ) is essentially the average value of  $r$  for the sheet and is independent of the planar anisotropy. Since the value of  $r$  varies continuously with change in direction in the sheet (Figure 4.20), it is sufficient to measure  $r$  only on specimens

parallel to and at  $45^\circ$  to the rolling and transverse directions. Thus the normal anisotropy,  $\bar{r}$ , is defined as (2,5,10,18,29,30)

$$\bar{r} = \frac{r_0 + 2r_{45} + r_{90}}{4}$$

Thus the  $\bar{r}$  value is independent of rational anisotropy in the plane of the sheet. When the  $\bar{r}$  value is greater than unity,  $\dot{\varepsilon}_t$  will be smaller than  $\dot{\varepsilon}_w$  on the average and thus the material has resistance to thinning. Unlike the planar anisotropy, normal anisotropy can be beneficial to the deep-drawing performance of the material. (5,16,33) It is possible to have a very high level of normal (thickness) anisotropy in a sheet with little or no planar (rotational) anisotropy.

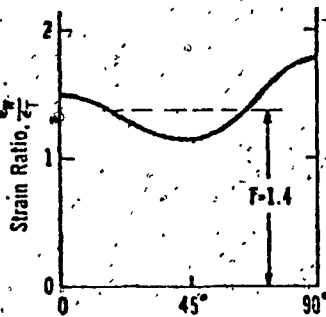


Figure 4.20 The normal anisotropy coefficient  
(From Ref. 10)

The practical importance of this "normal" anisotropy was not fully recognized for two reasons - the properties in the thickness direction can not be readily measured directly, and the effects of normal anisotropy are not visually evident, as in the case of earing. In fact, sheet-metals often exhibit a flow strength in their thickness direction quite different from that in their plane. (2,5,18,33) Typical  $\bar{r}$ -values for several common metals used in forming (5,10,32,33) are:-

Normalized steel	1.0
Rimmed steel	1.0 - 1.35
Aluminum-killed steel	1.35 - 2.0
Copper, brass	0.8 - 1.0
Aluminum	0.58 - 0.65
Lead	0.2
Hexagonal-close packed metals	3 - 6 +

#### 4.3.4 ISOTROPIC MATERIAL

A completely isotropic material has a strain ratio of unity for all directions of testing; furthermore,  $\Delta r = 0$  and  $\bar{r} = 1$  (Figure 4.21). It indicates equal flow strengths in the plane and thickness of the sheet-metal. Such a sheet has only fair drawability. (2,5,10)

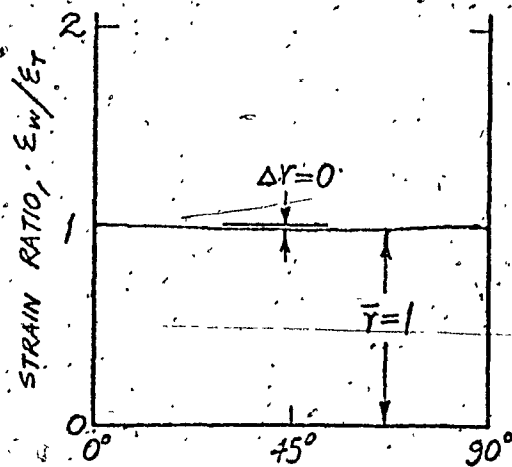


Figure 4.21 The isotropy expressed by  $\bar{r}$  and  $\Delta r$

The variation of the strain ratio ( $r$ ), with direction of testing reflects the degree of planar anisotropy present. The two parameters,  $\bar{r}$  and  $\Delta r$ , adequately define the plastic anisotropy of sheet-metal.

#### 4.3.5 FACTORS INFLUENCING ANISOTROPY

The degree of anisotropy is closely related to (a) the degree of preferred crystallographic orientation (10,33) and (b) the anisotropy of the individual grains which depends strongly on the crystal structure of the metal or alloy. In general, anisotropy develops more strongly in hexagonal-close-packed metals than the body-centered cubic metals.

Consider the body-centered-cubic structure of low-carbon steel. This structure, shown by Figure 4.22, is strongest when measured along the cube diagonal  $[111]$ , less strong along the face diagonal  $[011]$ , and weakest along the cube edge  $[001]$ . Thus, as more of the crystals in a sheet have a preferred orientation, the bulk sheet-metal takes on the anisotropic characteristics of a single crystal. The average strain ratio increases with the increased preferred orientation which results from greater cold reduction; this is illustrated in Figure 4.23 for sheets of aluminum-killed steel rolled to different reductions and annealed. (10) The strain ratio increases with increase of cube-on-corner component of the texture (in which the cube diagonal, or strongest direction, is oriented perpendicular to the sheet) and decrease in cube-on-face textural component (weak cube edge normal to sheet). For reductions greater than 75%, although the intensity of the cube-on-corner texture continues to rise until cold reductions top 90%, the average strain ratio drops off because of the increase in the cube-on-face textural component.

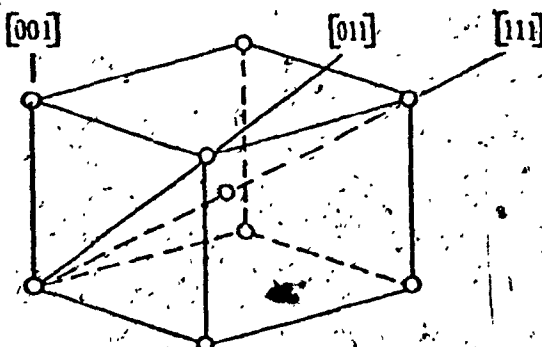


Figure 4.22. Body-centered-cubic lattice. (From Ref. 10).

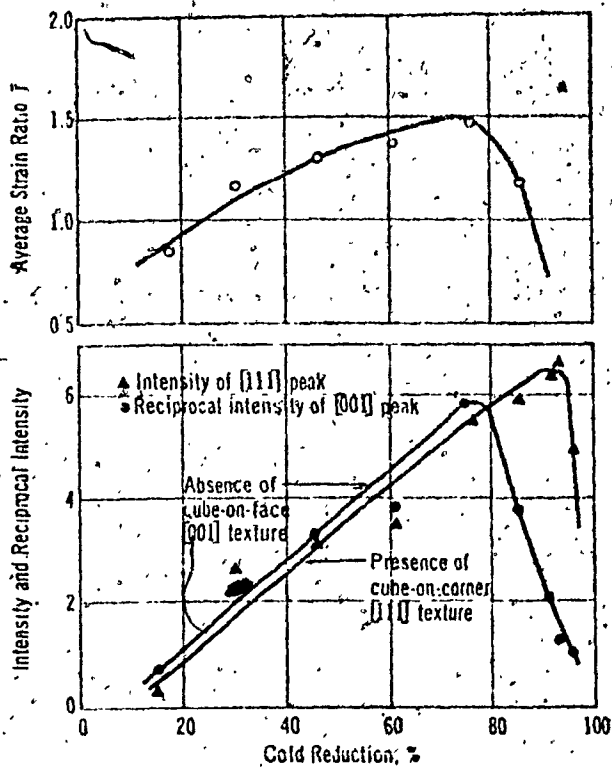


Figure 4.23 The average strain ratio and fine annealed texture vary with the amount of cold reduction. The increase preferred orientation is measured by the increase in the number of crystals with [111] perpendicular to the sheet which appears as an increase in intensity of [111] X-ray peak. (From Ref. 10).

For a given metal and composition, the degree of anisotropy is also dependent on its entire processing history. (10,33) The types and amounts of alloying elements also influence the nature of the anisotropy through changes in the texture produced for a given processing history. An excellent example is the effect of aluminum in increasing the anisotropy of aluminum-killed steel over that of the rimmed

steel. Witmer and Willison<sup>(4)</sup>, in evaluating the effect of nitrogen on aluminum-killed sheet steel, found that some added nitrogen, specifically in the 0.012 - 0.014% range, improve the  $\bar{E}$  value of 0.025% aluminum-killed sheet steel, although the ductility of the steel in general decreases with added nitrogen.

#### 4.3.5.1 MECHANICAL FIBERING

A second source of anisotropy is mechanical fibering. It is created when a material is rolled from an ingot to a sheet. Inclusions, segregation, porosity or other imperfections are all oriented and elongated parallel to the rolling direction. This anisotropy is non-crystallographic in origin and is present in varying degrees in all wrought materials. It affects the ultimate tensile strength and the ductility of the metal.

#### 4.3.6 EFFECT OF ANISOTROPY ON DEEP-DRAWING

The primary influence of anisotropy on metal formability is in deep-drawing. While planar anisotropy which produces earing during drawing is generally undesirable, another form of anisotropy, the normal anisotropy, can be

an asset to good drawability. (5,6,10,20,32,33) Earing is considered a liability in forming; a trimming operation is usually required, which limits the useful length of drawn cup walls. The thickness also varies being less in the ears.

Shop experience (10) and cup drawing test (5,20) show that earing behaviour is determined by the directional variations in  $r$ . The  $r$  value is plotted as a function of angle to the rolling direction, Figure 4.24. Ears occur in the directions in which  $r$  is a maximum. Figure 4.25 shows the directional variation in  $r$  for three low carbon steels. (5) All the low carbon steels exhibited ears at  $0^\circ$  and  $90^\circ$  to the rolling direction, and the only materials which do not ear (e.g. brass, copper and austenitic stainless steel) are those which show little or no directional variation in  $r$ . (5)

The height of the ears produced generally increases with increase in the degree of fluctuation in  $r$ , i.e. as  $\Delta r$  becomes greater (Figure 4.26). Willis and Blade (41) proposed as a measure of earing the difference between the average ear height and the average trough height expressed as percentages of the mean cup height.

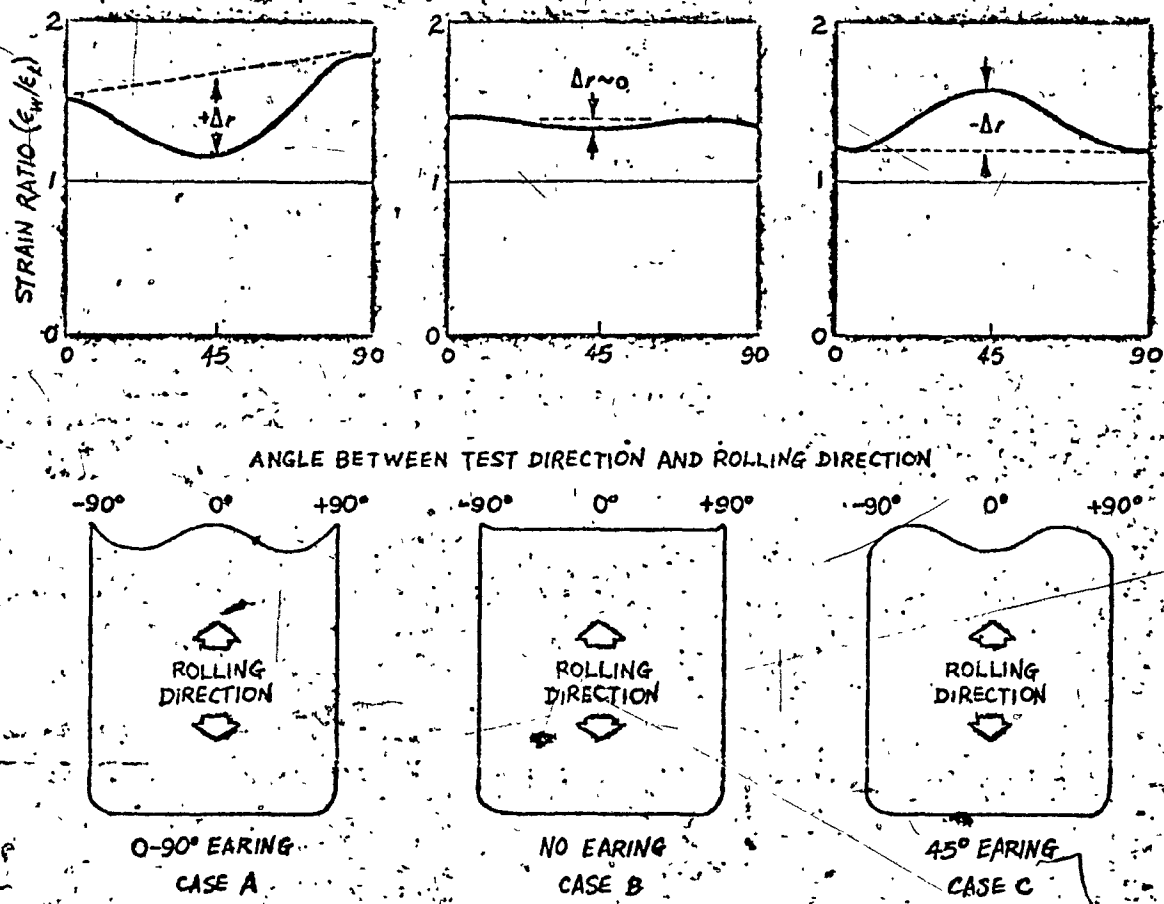


Figure 4.24 Earing of cups related to  $r$  values.  
(From Ref. 33)

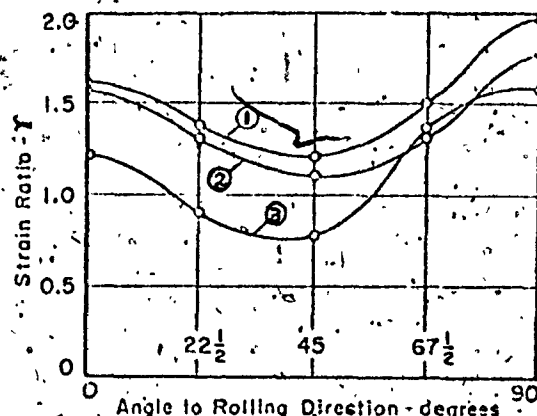


Figure 4.25 Typical directional variation of the strain ratio ( $r$ ) in the low carbon steels. Steels 1 and 2 are drawing quality aluminum-killed steels while steel 3 is a drawing quality rimmed steel.  
(From Ref. 5)

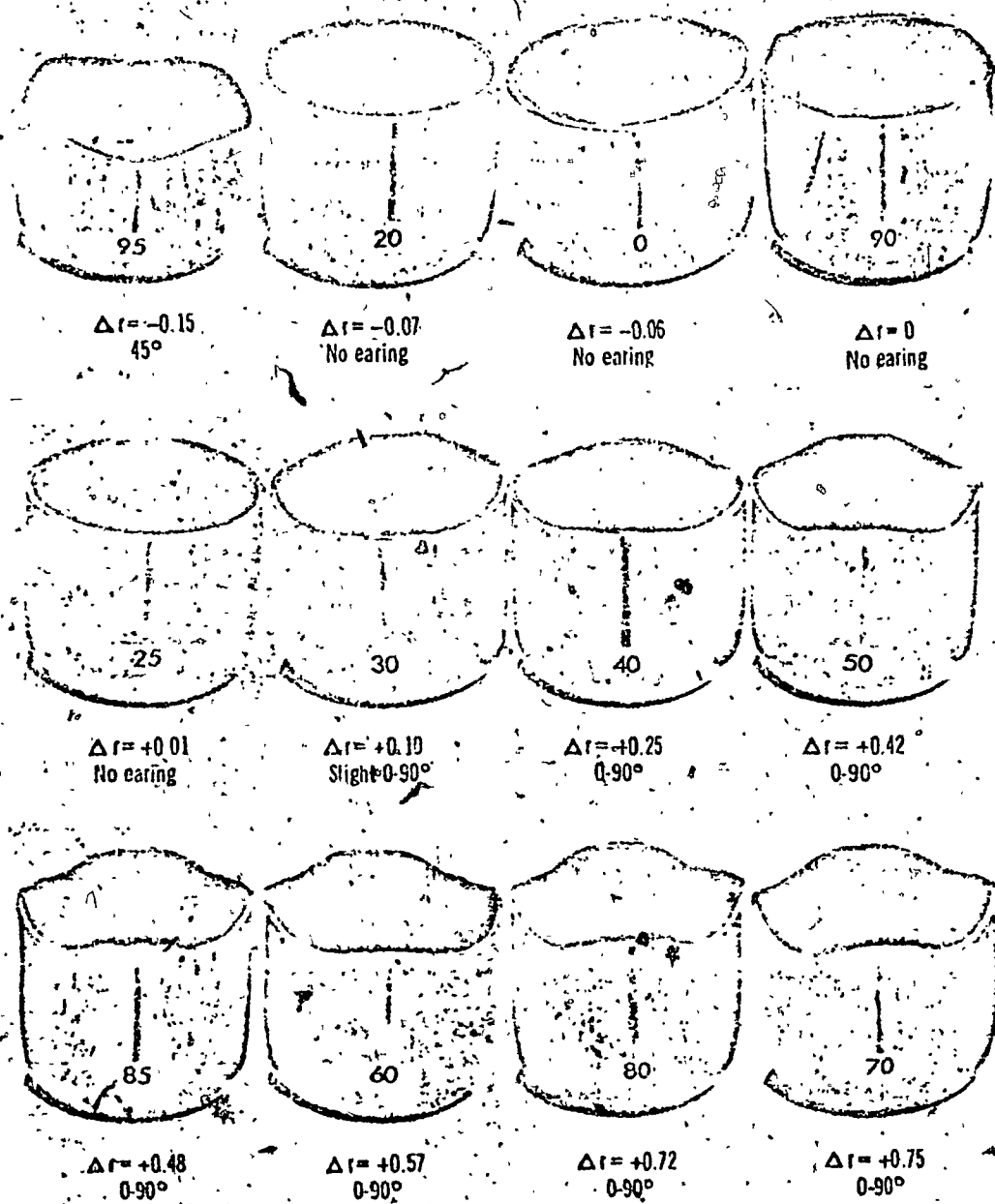


Figure 4.26. Earing behaviour varies with  $\Delta r$ . Vertical lines on caps mark rolling direction while the numbers indicate the percentages of cold reduction. (From Ref. 10)

In experiments to correlate deep-drawing performance in practical stamping operation tests with the strain ratio, the U.S.A. Committee of the International Deep Drawing Research Group<sup>(6)</sup> reported an increase in flange wrinkling for stamping blower housings with low strain ratio blanks. Thus, it appears that favourable anisotropy provides a smoother flow of metal during deep-drawing. The increased wrinkling with low  $r$  has been observed on other appliance parts where rimmed steel has been substituted for killed steel.

An average strain ratio of unity indicates that flow strengths are equal in the width and thickness of the specimen. If the strength normal to the sheet is greater than the average strength in the plane of the sheet, the average strain ratio ( $\bar{r}$ ) is greater than unity. Values of  $\bar{r}$  greater than unity then represent the anisotropic condition whereby longitudinal extension in uniaxial stretching is at the expense of a proportionately greater contraction in width than thickness; thus, in corresponding biaxial stretching thinning is resisted and drawability enhanced. A high average strain ratio, therefore, indicates that the sheet will resist thinning.<sup>(2,5,10,14,18,20,28,29,33)</sup> In the same manner, an  $\bar{r}$  value less than unity implies ease of thinning.

The higher the  $\bar{r}$  value, the deeper the cup that can be formed by deep-drawing. (2,6,10,14,16,28) Figure 4.27, for instance, demonstrates this relationship for several sheet metals.. (3,5,18,19,20,33) The drawability of the material is expressed as the ratio of the diameter of the largest blank successfully drawn to the diameter of the drawn cup. This ratio is called the Limiting Drawing Ratio, LDR. It will be noted that aluminum and other FCC metals are at the low end of the range where  $\bar{r}$  is one or less, while BCC mild steel and HCP titanium have higher  $\bar{r}$  values and greater drawing ratios.

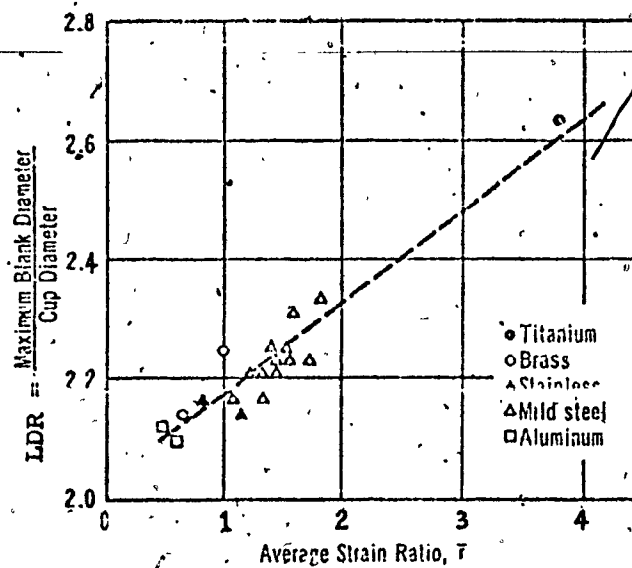


Figure 4.27 Effect of the average strain ratio on the limiting drawing ratio for several sheet metals (From Ref. 2, 5, 18, 19, 20, 32, 33).

A new steel, called Armco I-F steel, is reported by Armco Steel Corporation, U.S.A. to be a superior forming steel than aluminum-killed steel. Production evaluations confirmed that different parts drawn by I-F steel have fewer rejection rate than aluminum-killed steel. (42) The  $\bar{r}$  value of Armco I-F steel is 1.97. (43)

The drawability of several materials is compared on the basis of their  $\bar{r}$  values in Figure 4.28. (33) The  $\Delta r$  for all three cases is equal, indicating equal amounts of earing. However, the average  $\bar{r}$  level varies greatly. The lower the  $\bar{r}$ , the poorer the drawability. While most of the materials produced ears when drawn, the occurrence of earing did not appear to affect the relative drawability of the materials. Unfortunately, a material with high normal anisotropy usually has a high planar anisotropy as well. A typical example for aluminum-killed steel would show  $r_0 = 1.43$ ,  $r_{45} = 1.20$ ,  $r_{90} = 2.50$ ,  $\bar{r} = 1.58$  and  $\Delta r = +0.76$ . It would be an advantage in forming to have a sheet metal with a high  $\bar{r}$  value and a  $\Delta r$  value of zero.

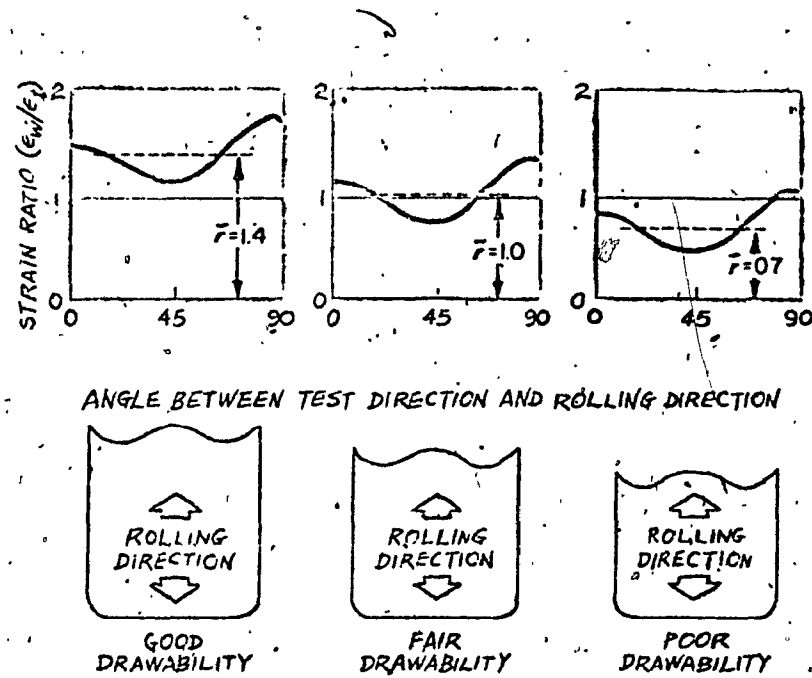


Figure 4.28 Deeper cups of flat-bottom cylindrical configuration can be drawn when  $\bar{r}$  values are high. The amount of earing is traceable to the variation of  $r$  with direction. (From Ref. 33)

#### 4.3.7 EFFECT OF ANISOTROPY ON STRETCHING

The influence of anisotropy on stretchability is very small compared to cup drawing and is illustrated by contradictory findings. More work should be expended to clarify this effect.

#### 4.4 CORRELATION OF STAMPING PERFORMANCE OF SHEET-METAL WITH WORK-HARDENING AND ANISOTROPY PROPERTIES

Interlaboratory tests conducted on practical stampings sponsored by the U.S.A. Committee of the International Deep Drawing Research Group<sup>(6)</sup> demonstrates the differences in dependence on  $\bar{r}$  and  $n$  of parts involving different degrees of drawing and stretching. The specimens were subjected to three stamping operations in the production of: a panel truck door, a blower housing, and an automotive instrument panel. Press quality was evaluated by the percentage of breakage occurring. The door panel, primarily a punch stretching operation, correlated best with  $n$  and showed little dependence on  $\bar{r}$ . The blower housing, predominately deep-drawn, correlated best with  $\bar{r}$ , and the instrument panel, in which combination of stretching and deep-drawing are appreciable, showed a strong dependence on both  $n$  and  $\bar{r}$ . Figure 4.29 clearly illustrates the three types of correlation obtained.

Many workers<sup>(2,5,7,11,13,20,28,29,30)</sup> draw similar conclusions in the correlations between stamping operations and  $n$  and  $\bar{r}$  values.

Another example, as shown in Figure 4.30, demonstrates the results obtained when a car fender pressing is assessed.<sup>(32)</sup> It shows that below  $\bar{r} = 1.5$  and  $n = 0.24$  - both values arbitrarily fixed - 24 out of 29 have failed, while above this standard 14 of the 17 lots come up to the requirements.

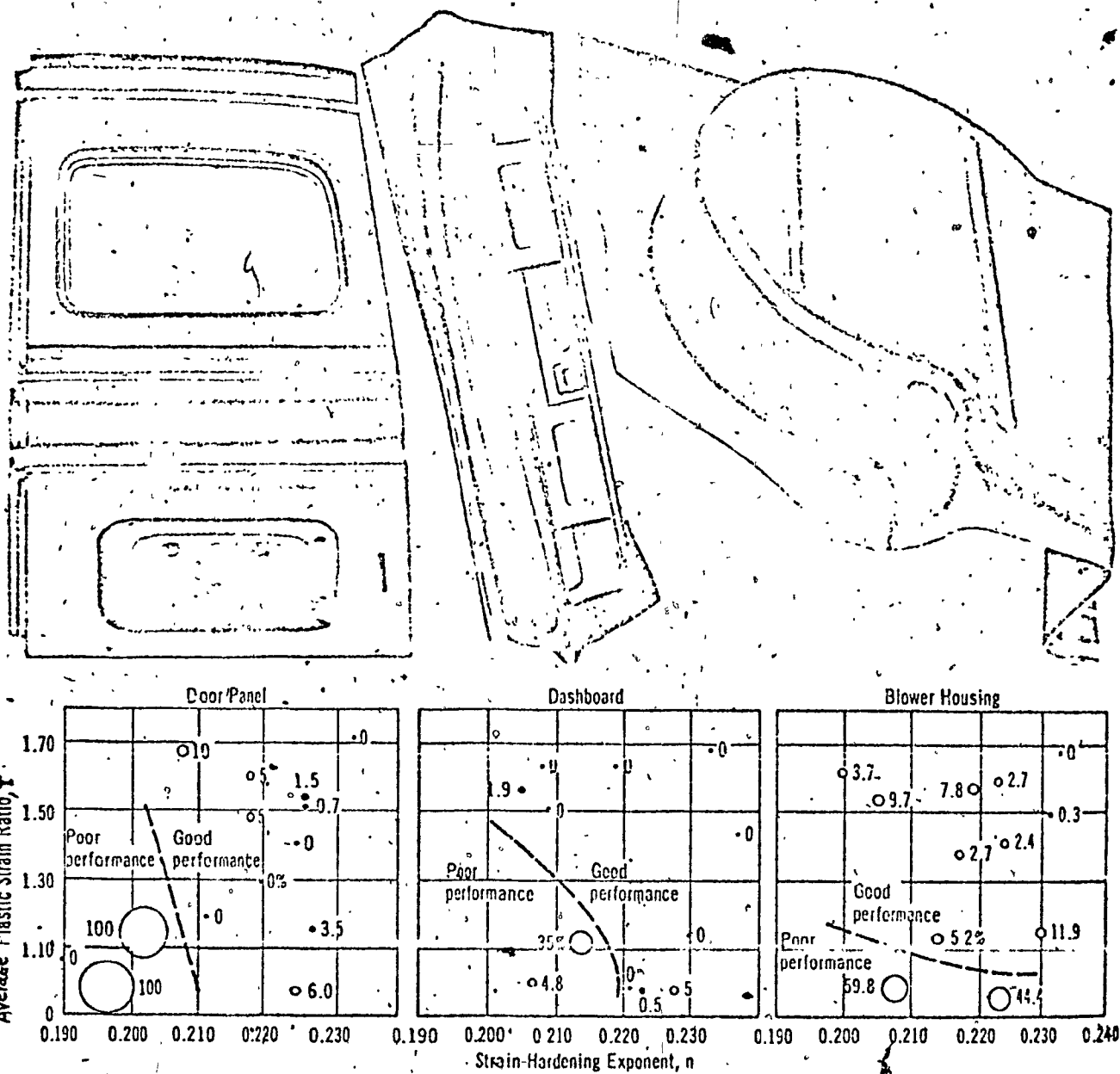


Figure 4.29 Parts that are formed largely by stretching (left) should have a high strain-hardening exponent; those that are drawn (right) need a high average strain ratio; and those shaped by both actions (centre) require both properties to be high. Percentages refer to scrap rate. (From Ref. 2, 6)

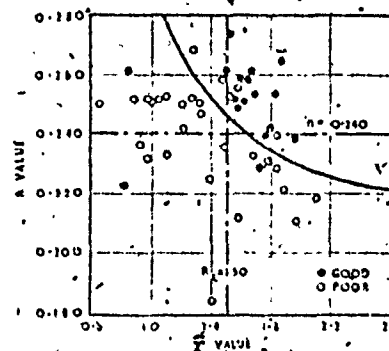


Figure 4.30  $n$  value versus  $\bar{r}$  value for all lots tested.  
(From Ref. 32)

## CHAPTER 5

### EFFECTS OF VARIABLES AND APPLICATION OF FORMING LIMIT DIAGRAM ON THE IMPROVEMENT OF FORMABILITY

#### 5.1 GENERAL APPROACH FOR SATISFACTORY STAMPING

A part design may be in the critical class and still yield good stampings during the trial stage. However, when the part is in production, there may be a substantial increase in the breakage rate. Any one of a multitude of variables might have changed the performance in stamping: press speed, die design, die alignment, lubrication, stamping geometry, blank configuration, or material properties. Proper use of strain analysis would permit detection of a critical stamping in the tryout stage, even though stampings have been made without breakage. Such an evaluation would indicate a need for further die or press operation modification or a revision of the steel specifications. Thus strain distribution analysis can result in direct and tangible benefits, mainly the reduction of production breakage.

The Forming Limit Diagram (FLD) can be used at all stages of press manufacture to systematically remedy failures and to determine the optimum material properties, lubrication conditions and die-setting for a given stamping. A systematic remedial method of analysis has been applied successfully by the Manufacturing Development Department, Austin-Morris Body Plant, British Leyland Motor Corporation, England for die try-out strain analysis. (22)

- (a) Produce a laboratory forming limit diagram as a material standard.
- (b) Press a gridded sheet.
- (c) Measure and calculate the major and minor strains in the critical region; and consult the FLD.
- (d) If the stamping is split, the material is not capable of withstanding the local strain combination. Blank-holder pressure, lubrication, design, and sheet metal may be systematically altered to modify the strain state.
- (e) If the stamping is successful, the part could become a reference standard for the rest of the run and for subsequent runs. If the stamping is successful with too large a safety factor, economy may be effected by changing to a less ductile, cheaper grade of sheet.

The most effective method of increasing stretchability and drawability is the development of a more nearly uniform strain distribution under the critical strain limit. From a practical point of view, increase in the depth of the stamping without failure can be achieved primarily through reduction of the peak strain by redistributing the strain more uniformly throughout the stamping. Smoothing out the strain distribution also reduces the normal strain reducing thinning. A greater capacity for strain hardening renders a material more suitable for stamping by making deformation more uniform. Such a material has a high  $n$  value, a large uniform elongation and a high tensile/yield stress ratio. Mechanically, strain distribution is controlled strongly by lubrication, tool and die design and press variables.

The strain distributions of two materials strained to the critical strain limit is shown schematically in Figure 5.1. The depth of stamping is proportional to the average strain value of the stamping, which in turn is related to the area under the curve. Material A has greater depth at failure because the more nearly uniform strain distribution permits a greater average strain. Material B has a very localized deformation. Conversely, if two stampings are at the same depth, this is indicated by equal areas under the two curves, as shown in Figure 5.2. The stamping B with the most nearly uniform strain distribution will have the lowest maximum peak strain. This stamping, in turn, will have the greatest relative safety factor and the smallest chance of breakage.

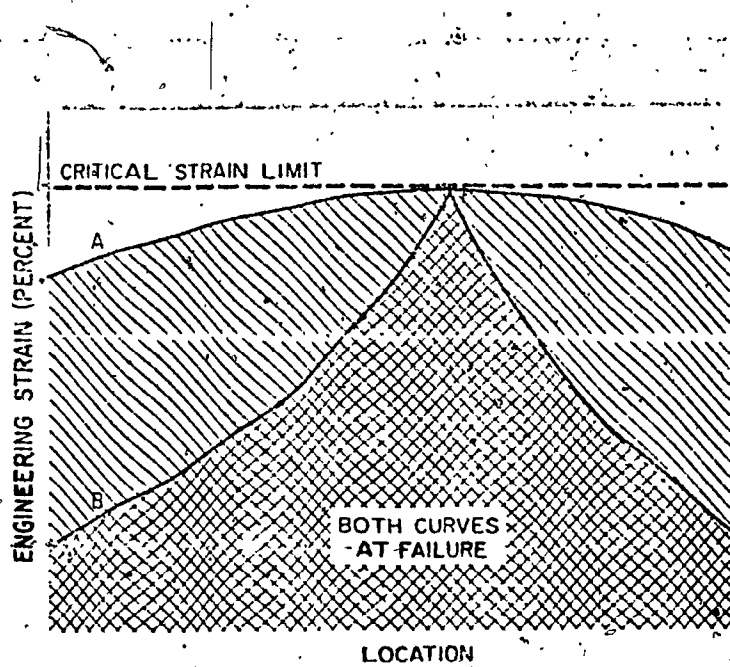


Figure 5.1. Schematic strain distributions of two materials strained to the critical strain limit.  
(From Ref. 33)

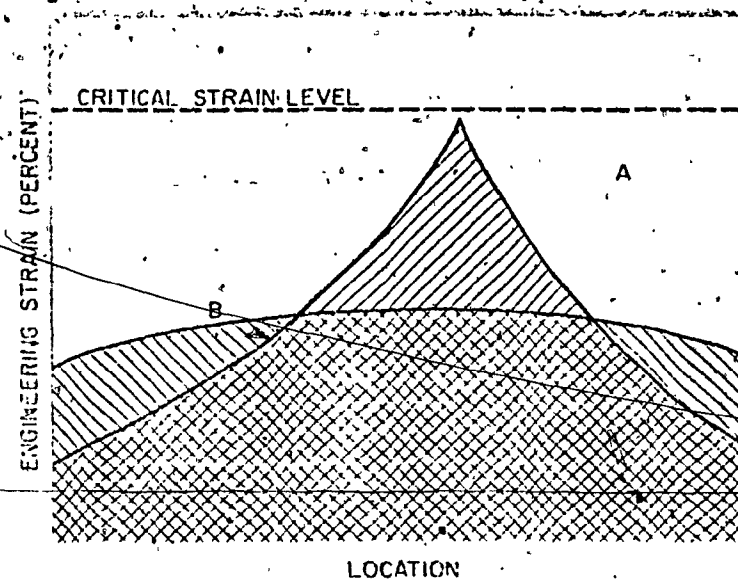


Figure 5.2. Schematic strain distribution for two materials stretched to the same depth. (From Ref. 33)

### 5.2 CHARACTERISTICS OF MATERIAL AFFECTING STAMPING

Although anisotropy and work-hardening capacity are the principal properties that determine a sheet's press performance, other properties are also significant. In general, the higher the ductility as shown by the tensile test, and the lower the hardness, the more a material can be deformed without fracture. An exceptionally clean material might have a higher failure forming limit than material containing preferential failure sites, such as large inclusions and internal cracks.

### 5.2.1 INFLUENCES OF YIELD STRESS

A low yield point is an important fundamental property from a metal-forming viewpoint. (2,32,33) The yield point decreases with diminishing deformation speed. For plastic flow to occur over the punch nose as illustrated in Figure 5.3, tensile stresses are induced in the sheet near the blankholder. Failure could occur in this region if too high a load is required to bring about plastic flow over the punch.

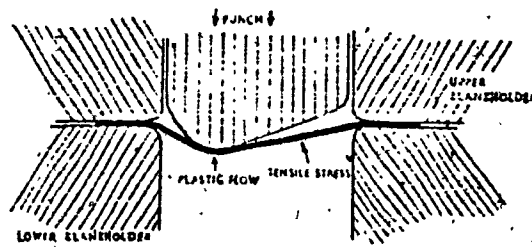


Figure 5.3: The danger of failure due to exceeding the breaking-load when forming. (From Ref. 32)

### 5.2.2 DISADVANTAGE OF YIELD-POINT ELONGATION

If a sheet has a double yield point and a large yield point elongation, slightly deformed areas of a stamping show surface markings called Lüder's lines (stretcher strains or Piobert lines). They disfigure the surface, and may cause rejection of stampings for exterior parts of automobiles, appliances, and the like. The severity

of the defect is related directly to the extent of yield point elongation. (1,2) Occasionally stampings fail at a very low total strain because fracture is initiated within the Lüder's bands and the larger part of the metal does not contribute to the total strain. (33)

#### 5.2.3 EFFECT OF GRAIN SIZE

A fine grained steel can be deformed to a greater extent

than a coarse-grained because it has a higher  $n$  value. (1)

The surface of the fine-grained steel is smooth after cupping in comparison with a coarse-grained material which has a crinkled 'orange peel' surface.

#### 5.2.4 EFFECTS OF PRIOR COLD WORK

Cold working of the sheet greatly reduces its formability in two ways, (33,36) as indicated by the schematic drawing in Figure 5.4. First, the total amount of usable strain a material can undergo before failure is reduced; this lowers the critical strain limit. Second, cold working reduces the strain hardening because its coefficient causing the strain distribution to become more non-uniform in the presence of a stress gradient. The critical strain curve and the peak strain value rapidly approach each other as the prior deformation increases indicating a strong reduction

in the formability of the material. The disadvantage of cold work is also illustrated in Figure 4.16.

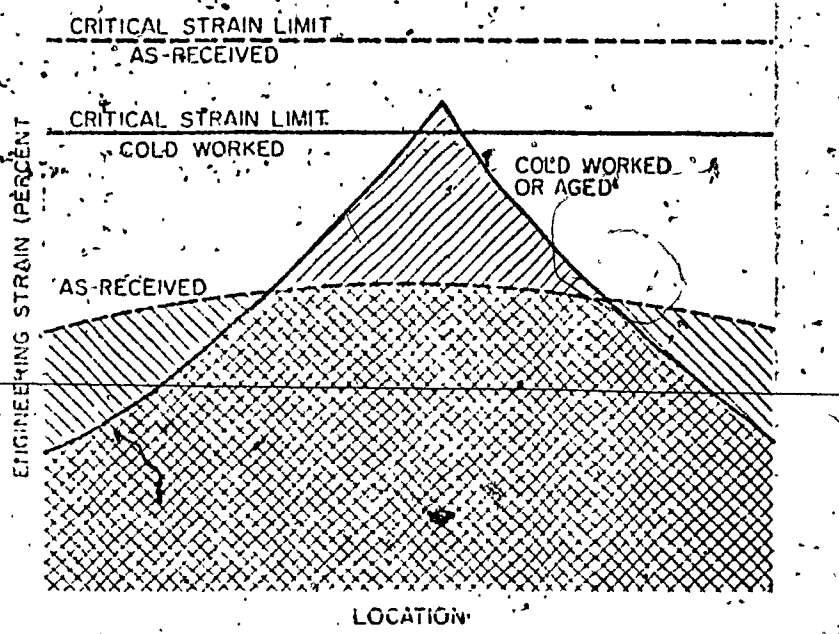


Figure 5.4. Effects of cold work on the forming capacity of a metal before failure. (From Ref. 33)

#### 5.2.5 EFFECT OF STRAIN AGING

Aging after cold working of the sheet causes the yield strength to increase, resulting in a reduction in both the tensile-yield stress ratio and the work-hardening coefficient. (25,33) Aging also causes the yield point elongation to increase. Figure 5.5 shows that aging of a rimmed steel lowers the critical strain limit slightly. (25)

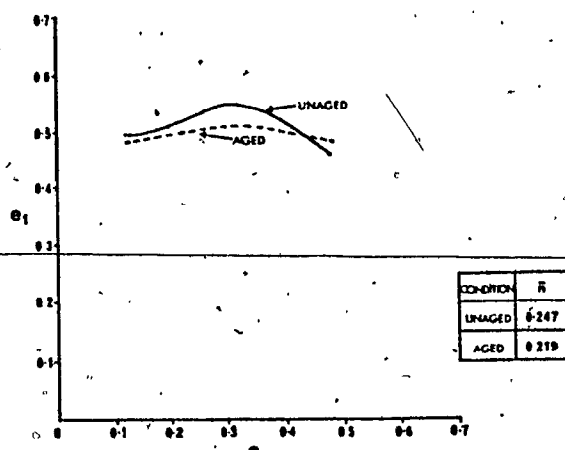


Figure 5.5. Forming Limit diagrams for 0.036 in. rimmed steel in the unaged and aged conditions. (From Ref. 25)

#### 5.2.6 EFFECTS OF SURFACE SCRATCH OR SUBSURFACE LAMINATION AND BURR

A surface scratch or subsurface lamination can act as a stress raiser and lead to premature failure. This is especially true when the imperfection is on the tension side of a bending specimen. Many breakage problems are created by tension along a blanked or sheared edge as a result of the reduced ductility at a heavily worked margin zone or burr which is the result of dull shearing.

knives or incorrect clearances. When the heavily worked zone is subjected to high strain, a crack can develop. The empirical relationship between elongation at fracture and burr height (33) is shown in Figure 5.6. Burrs of various heights were generated by shearing long strips with incorrectly set blades. Values of percent elongation at the onset of fracture are obtained from tensile tests of specimens having one sheared edge. A slight burr reduces the permissible percent elongation severely.

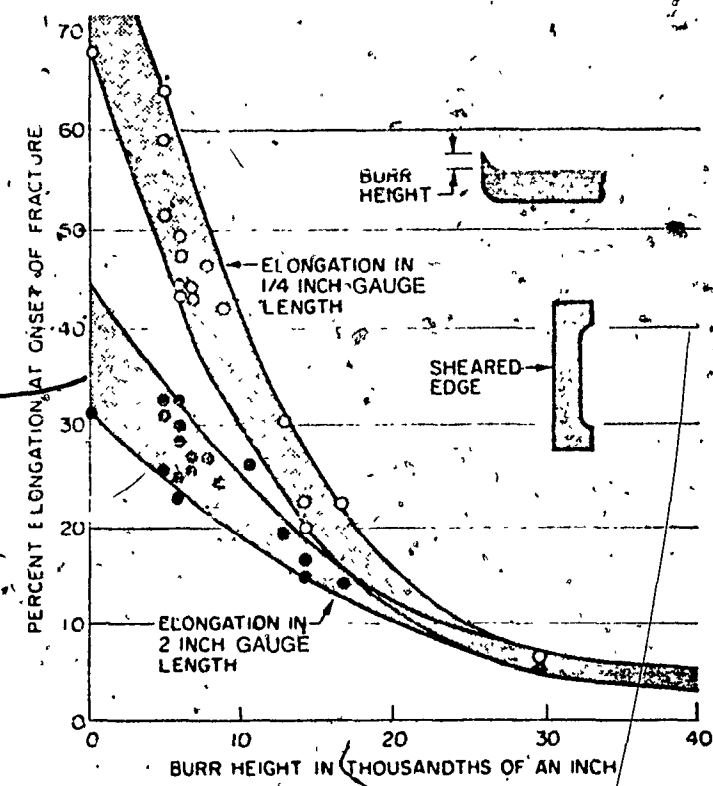


Figure 5.6. Effect to elongation at fracture by burr from poor blanking operation. (From Ref. 33).

The blanked edge of an automotive outer frame member tore during forming at two places where there were severe edge elongations caused by burrs. The strain distribution is shown in Figure 5.7. Apart from the remedies, such as improving the sheared edge, filing off the burrs and edge annealing, an unusual technique (33) is to file notches into the edge of the blank at points of low strain at the edge of the tears (A and B as shown in the Figure). The result is a general smoothing out of the strain distribution and a reduction of the peak strain. Notching devices can be built into blanking dies.

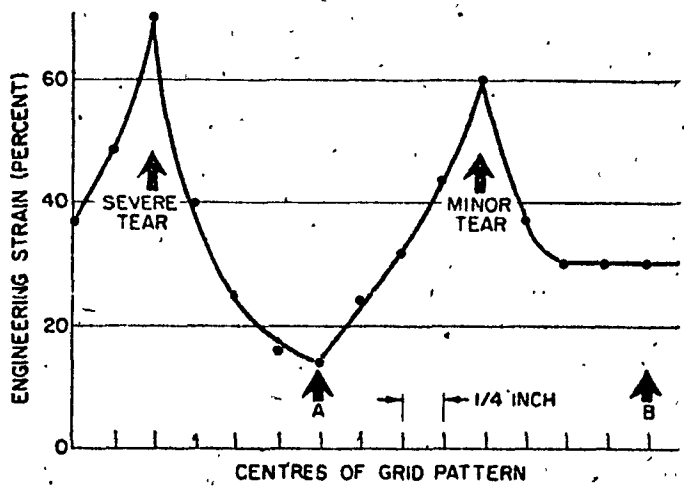


Figure 5.7: Strain distribution along the edge of an automotive outer frame member. Two tears are associated with the peak strains. (From Ref. 33)

### 5.2.7 ADVANTAGES OF COATING ON METAL BLANK

The Swift cupping tests (Figure 5.8) of Duckett, Barry and Robins (23) showed that tin coatings as thin as  $0.08 \times 10^{-3}$  mm improved the drawability. The limiting drawing ratio of mild steel sheet was progressively increased by thicker coatings of tin up to  $0.8 \times 10^{-3}$  mm. This is true for steel plated on both faces and steel plated on one face only, provided that the tin is in contact with the die, on the face away from the punch. A tin coating in the absence of an oil film increases the drawability of the steel because the tin itself acts as a SOLID lubricant. A tin coating in the presence of an oil film has an even more beneficial effect.

Phosphate coatings improve deep drawability in reducing the punch load about 14 percent, as compared to bare metal. (35)

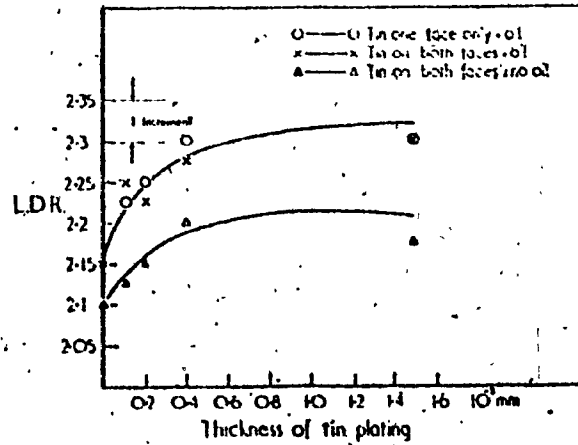


Figure 5.8. Effect of tin coating thickness on the LDR of deep drawing mild steel sheet, both lubricated and unlubricated. (From Ref. 23)

### 5.3 EFFECT OF FORMING RADIUS IN PART DESIGN

The strain gradient, or non-uniformity of the strain distribution is strongly dependent on the radius over which the sheet is stretched. (9, 28, 33) The smaller the radius, the more localized the peak strain and the greater possibility of breakage. In practice, considerable additional depth before fracture can be obtained from a very small increase in punch radius of curvature. Sometimes removal of 1/32 inch off the point of a punch is sufficient.

A comparison is made in Figure 5.9 between the strain distributions developed over a 2-in. and a 4-in. diameter hemispherical laboratory punch and a die with 4 inches opening. (28, 33) The larger punch distributes the strain over a greater area and increases the permissible depth before failure.

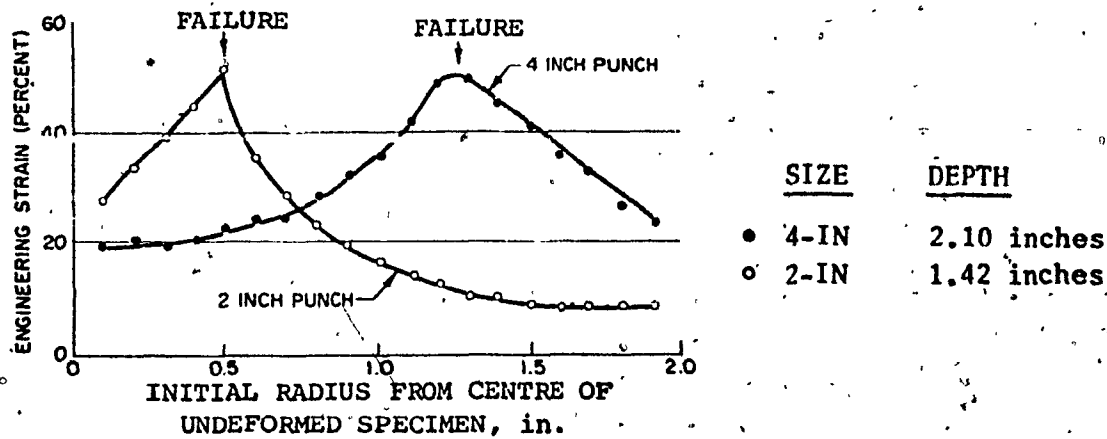


Figure 5.9 Distribution of principal strain at maximum (failure) depth in lubricated, annealed steel discs securely clamped and stretched over hemispherical punches of varying diameter. (From Ref. 28, 33).

A significant reduction in punch force is also achieved as the die radius is increased. (35) The reduction of the total punch force reduces the thinning of the cup wall in deep-drawing. Increase of the die radius can also reduce the breakage.

#### 5.4 INFLUENCES OF PRESS OPERATING CONDITIONS

##### 5.4.1 EFFECTS OF LUBRICATION AND FRICTION

The degree and type of lubrication can strongly influence the strain distribution. Metal flow is assisted by lubrication and discouraged by friction; the amount of lubrication desired varies with the geometry of the stamping and will be discussed below. The effectiveness of a lubricant depends on forming speed, interface pressure, material surface condition, die design and many other factors. In many cases the selection of a particular lubricant is dictated not by its lubricating ability but by its compatibility with other operations.

The effectiveness of a lubricant change in making the strain distribution more uniform was reported by Goodwin.

(12) As shown in Figure 5.10, strain measurements made on the leading edges of production automotive hood panels produced from rimmed steel showed a reduction in peak strain from 50 percent to 20 percent when one lubricant was sub-

stituted for another. As a result of the change of lubrication, the expensive change to other material or die modification is avoided.

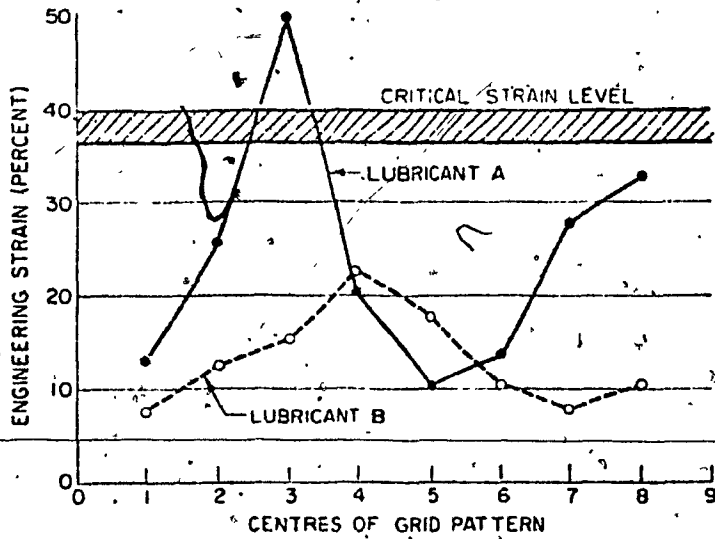


Figure 5.10 Effect of lubricants on major strains.  
(From Ref. 12, 33).

Dry polyethylene sheet has been found to be a very good lubricant in stretch-forming test by many workers. (9,13,18,34) It improves the depth to which a part could be formed before failure. The relationships between average strain-ratio and limiting blank diameter in cupping tests with oil and dry polythene sheet were compared by Atkinson and MacLean (Figure 5.11). (18) Polythene gives the higher and more consistent values of limiting blank diameter throughout. Furthermore, plastic films are less susceptible than oil to variations in lubrication behaviour caused by surface roughness.

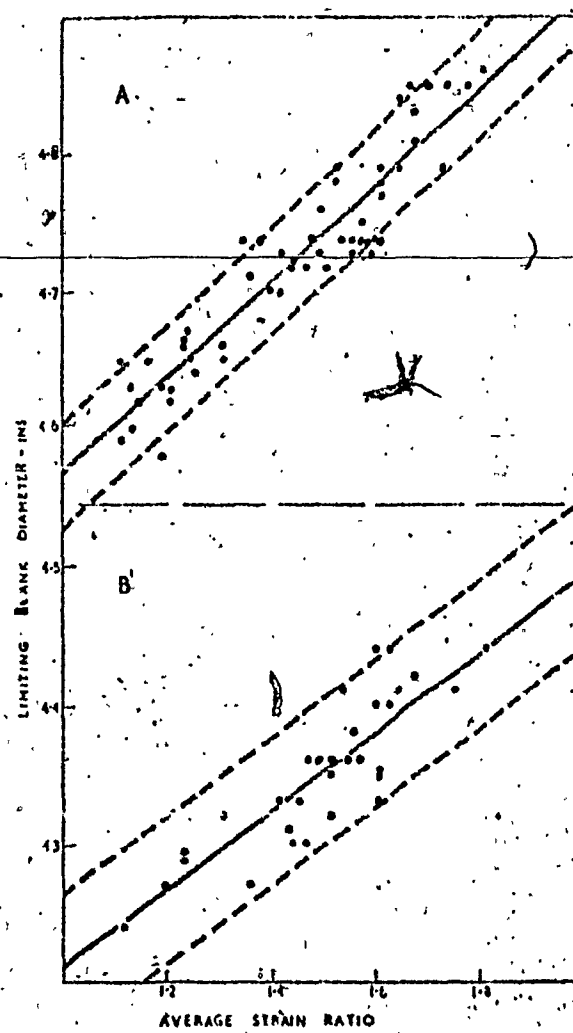


Figure 5.11 Relationship between limiting blank diameter and average strain ratio for A, polythene-film lubrication and B, Esso Oil TSD 996 lubrication. (From Ref. 18)

#### 5.4.1.1 LUBRICATION IN DEEP-DRAWING

In deep-drawing, punch lubrication is generally undesirable. High friction at a position such as W in Figure 5.12 inhibits metal flow, reduces thinning preventing instability. Thus the production of deep-drawn flat-bottomed cups with sharp radii is assisted by high friction over the punch nose. The complement to this is low friction between the die and blank holder (v in Figure 5.12) which reduces thinning due to bending under-tension by reducing the applied tension,

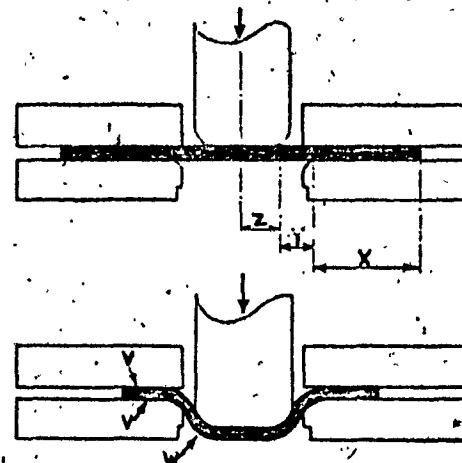


Figure 5.12 Drawing an axisymmetrical cup from a circular metal blank. (From Ref. 34).

#### 5.4.1.2 ADVANTAGE OF LUBRICATION IN STRETCHING OVER A LARGE RADIUS PUNCH

Good lubrication aids in stretching material over a large radius punch. Strain distributions in Figure 5.13 are obtained by stretching clamped discs over a 4-in. diameter hemispherical punch. (28,33) The lubrication permits metal in contact with the punch to deform and slide over the punch, reducing the localization of strain, thereby increasing the total depth of the stamping at breakage.

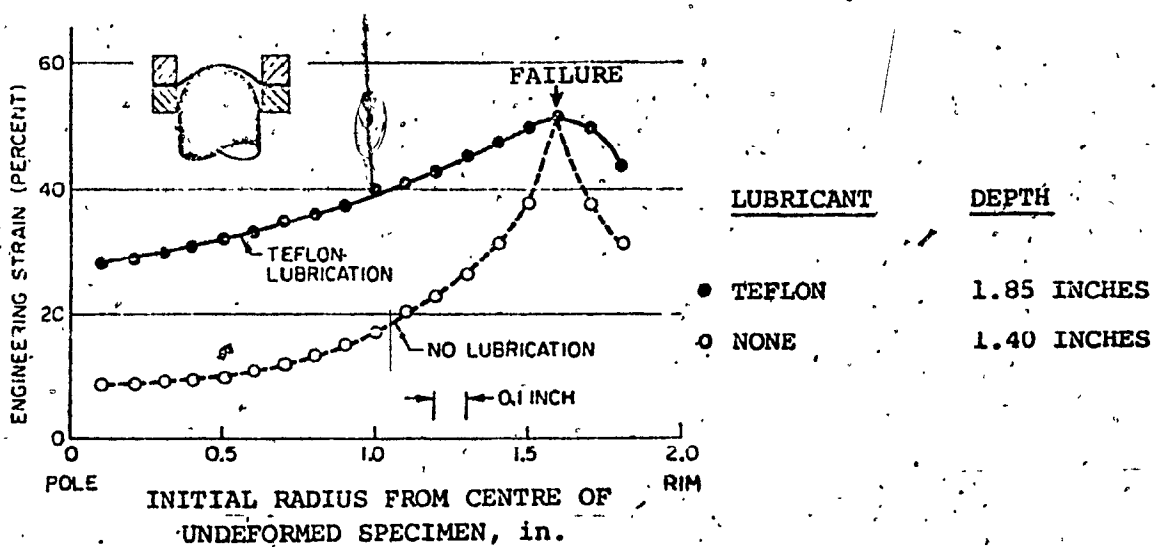


Figure 5.13 Distribution of principal strain at maximum (failure) depth in annealed brass discs after stretching.  
(From Ref. 28, 33).

#### 5.4.1.3 ADVANTAGE OF FRICTION IN STRETCHING OVER A SMALL RADIUS PUNCH

When the punch radius is small, high punch friction can produce a better part. (28, 33) Figure 5.14 illustrates the different strain distributions observed in a bumper stamping formed by a combination of stretch and draw. When a piece of emery tape is either absent or present between the sheet and punch at the high strain location. The increased friction at the sharp radius acts to retard strain at that location and causes the strain to be redistributed to other locations; more metal is also drawn in from the flange area. In a production situation, the emery tape is replaced by roughening the punch in selected areas.

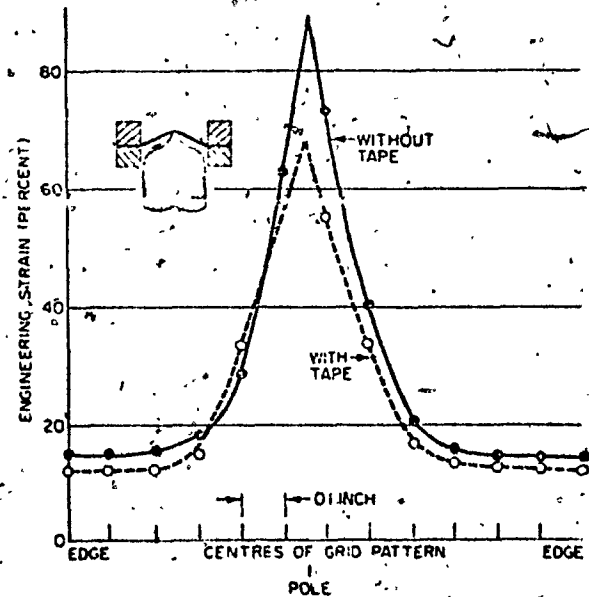


Figure 5.14 Small radius localizes strain. The peak strain is reduced by restricting metal flow in high strain region.  
(From Ref. 33)

#### 5.4.1.4 EFFECT OF BLANK SURFACE ROUGHNESS

Effects similar to those of lubrication and friction are obtained by varying the surface roughness of the metal blank. (28,33) An unlubricated rough surface has high friction which retards the metal being drawn in from the flange, and gives rise to higher strains in the punch stretching region. On the other hand, a rough surface can entrap and carry more lubrication into the deformation zone, thereby reducing the friction and non-uniformity of the strain distribution. A smooth surface initially has low friction; but if it is too smooth, it will not retain sufficient lubricant to cover newly generated surface area.

#### 5.4.2 EFFECTS OF PAD OR BLANK-HOLDER PRESSURE

The imposition of the correct blankholder pressure is important to stamping. (6,33,34) Too little blankholder pressure allows wrinkling; too much increases the stress during bending-under-tension over the die radius which result in increased thinning. Restriction of metal flow into the die opening due to wrinkling, excessive blankholder pressure or too large a blank can cause the cup

to tear at the punch radius. Unexpectedly, the blankholder pressure has no effect on punch load. (35)

The effect of blankholder pressure can be illustrated in the forming of an automotive panel<sup>(33)</sup> as shown in Figure 5.15. After successfully forming the steel in the first trial, the blankholder pressure was increased in the second trial which gave rise to higher strain levels and fracture of all the stampings.

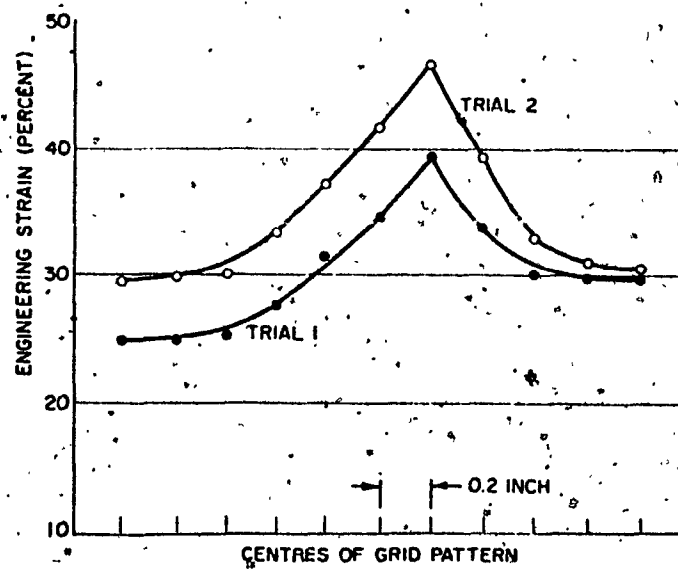


Figure 5.15. Increased blankholder pressure caused the strain to increase during forming of an automotive panel. (From Ref. 33)

#### 5.4.3 EFFECTS OF PUNCH FORMING SPEED

A stamping formed satisfactorily on a low-speed press may be completely unsatisfactory when formed on a high-speed.

press. Yield stress increases with deformation speed, tensile strength also increases but to a lesser degree. Formability of the sheet, if measured by the tensile to yield stress ratio, therefore decreases when speed increases. Furthermore, the yield point elongation of the material increases. Although punch force does not change significantly as the punch speed is increases, vibrations may be superimposed on the average punch force. Changes in the characteristics of lubricants with speed and temperature may influence formability. Cups drawn at high speeds were much hotter than cups drawn at low speeds, indicating that lubrication was more critical.

#### 5.4.4 PROBLEMS IN MULTISTAGE FORMING OPERATIONS

For stampings formed in a multistage operation in which the final shape and dimensions are established in a re-strike die, formability can be improved by minimizing the non-uniformity of strain distributions in the first draw. If the first draw has a sharply radiused, pointed punch over which the whole blank must be drawn to shape; strains will be severely localized. Once a peak strain condition has been generated, the non-uniformity of strain will increase in subsequent operations, often to the critical level. Such a condition is vividly illustrated in a brake backing plate (14,28,33) as shown in Figure 5.16.

Modification of dies in an early operation is usually easier and more beneficial than in subsequent operations. In early operations, more metal is available from the flange or other location for re-location into the critical area. Sufficient metal should be collected in each region of the primary pressing to form the final impressions of these regions in the re-strike operation.

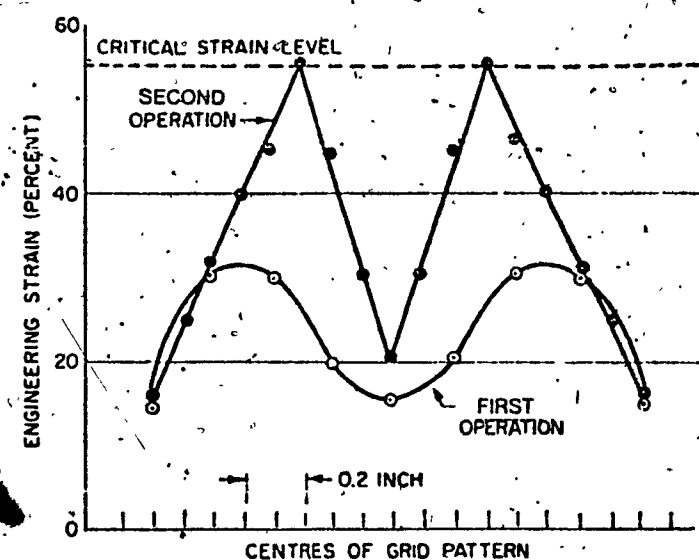


Figure 5.16 Distribution of principal strains across a dome formed during the first and second operations in producing a brake backing plate show that critical strains develop rapidly. (From Ref. 14, 28, 33).

CHAPTER 6CONCLUSIONS

The suitability of sheet-metal for pressing is a common goal that has long occupied the attention of both producers of rolled strip and fabricators of deep-drawn and stretched sheet products.

Simple mechanical tests that have proven satisfactory in determining the behaviour of the metal during fabrication are the work-hardening exponent ( $n$ ) and the plastic anisotropy coefficient ( $r$ ). For manufacturers of rolled sheet, these provide a reliable index to the suitability of sheet for pressing operations.

Production engineers and tool designers have need to determine the formability level required for each new stamping. Through evaluation of the strains imposed on the sheet during stamping by means of the circular grid system and through use of the Forming Limit Diagram which indicates the limit strains achievable, it is possible to determine the combination of material properties and stamping variables that is most favourable and economical for a particular stamping.

REFERENCES

- (1) Frank. T. Sisco, Modern Metallurgy for Engineers, Second Edition. Pitman Publishing Corporation, pp 172-178.
- (2) Donald J. Blickwede, Influence of Mill Processing on Metallurgy Formability. Metal Progress, 1968, Vol. 94, No. 6, pp 64-70.
- (3) R.H. Heyer and J.R. Newby, Measurement of Strain Hardening and Plastic Strain Ratio using the Circle-Arc Specimen. Sheet Metal Industries, 1966, Vol. 43, No. 476, pp 910-914.
- (4) D.A. Witmer and R.M. Willison, Effect of Nitrogen on the Mechanical Properties of Drawing-Quality Aluminum-Killed Sheet Steel. Journal of Metals, 1970, Vol. 22, No. 4, pp 56-62.
- (5) R.L. Whitely, The Importance of Directionality in Drawing Quality Sheet Steel. Transactions of the ASM 1960, Vol. 52, pp 154-163.
- (6) "Report on Cooperative Research of the U.S.A. Committee on the International Deep-Drawing Research Group", correlation of Deep-Drawing Press Performance with Tensile Properties, ASTM STP 390, American Society for Testing and Materials, 1965.
- (7) R.D. Jenkins & D.V. Wilson, The Characterization of Stretch-forming Behaviour by Measurement of Uniform Elongation in the Tensile Test. Sheet Metal Industries, 1971, Vol 48, No. 1, pp 21-24 & 38.
- (8) Arthur S. Kasper, How Steels and Dies Interact in Forming Shapes. Metal Progress, 1971, Vol. 99, No. 5, pp. 57-60.
- (9) David A. Chatfield & Stuart P. Keeler, Designing for Formability, Metal Progress, 1971, Vol. 99, No. 5, pp. 60-63.
- (10) Roger L. Whitely, How Crystallographic Texture Controls Drawability. Metal Progress, 1968, Vol. 94, No. 5, pp 81-84.

- (11) R. Pearce & D. Ganguli, The Forming Limits of Aluminum-Magnesium Alloy Sheet in Biaxial Tension. Journal of The Institute of Metals, 1972, Vol. 100, pp. 289-295.
- (12) Gorton M. Goodwin, Application of Strain Analysis to Sheet Metal Forming Problems in the Press Shop. SAE Paper No. 680093, SAE Transactions, 1968, Vol. 77, Section 1, pp. 380-387.
- (13) R.H. Heyer and J.R. Newby, Effects of Mechanical Properties on Biaxial Stretchability of Low Carbon Steels. SAE Paper No. 680094, SAE Transactions, 1968, Vol. 77, Section 1, pp. 388-396.
- (14) Stuart P. Keefer, Rating the Formability of Sheet Metal. Metal Progress, 1966, Vol. 90, No. 4, pp. 148-153.
- (15) John Woodthorpe & Roger Pearce, The Effect of r and n upon The Forming Limit Diagrams of Sheet Steel. Sheet Metal Industries, 1969, Vol. 46, No. 12, pp. 1061-1067.
- (16) Robert H. Heyer & John R. Newby, Factors in Selecting Materials for Forming. Metal Progress, 1967, Vol. 91, No. 3, pp. 85-88.
- (17) S.P. Lafferty, F.E. Schmidt and A. Lawley, In-Situ Determination of the R-Value in Sheet Tensile Testing. Sheet Metal Industries, 1971, Vol. 48, No. 3, pp. 185-188.
- (18) M. Atkinson and I.M. MacLean, The Measurement of Normal Plastic Anisotropy in Sheet Steel. Sheet Metal Industries, 1965, Vol. 42, No. 456, pp. 290-298.
- (19) Roger Pearce, an Introduction to the Forming of the 'Difficult' Metals. Sheet Metal Industries, 1965, Vol. 42, No. 459, pp. 490-496.
- (20) R.W. Rogers, Jnr. and W.A. Anderson, Effect of Plastic Anisotropy on Drawing Characteristics of Aluminum Alloy Sheet. Metal Forming: Interrelation between Theory and Practice; The Metallurgical Society of AIME Proceedings of a Symposium on the Relation Between Theory and Practice of Metal Forming, Held in Cleveland, Ohio, in October, 1970. Edited by A.L. Hoffmanner, Plenum Press, 1971, pp 185-198.

- (21) J.R. Branson, Grid Line Networks for Strain Measurement. Sheet Metal Industries, 1972, Vol. 49, No. 7, pp. 467-469.
- (22) I.C. Brookes and G.M. Davies, Gridmarking Techniques in the Press Shop. Sheet Metal Industries, 1972, Vol. 49, No. 11, pp. 707-710.
- (23) R. Duckett, B.T.K. Barry and D.A. Robins, Effect of Tin Coatings on the Drawability of Steel Sheet. Sheet Metal Industries, 1968, Vol. 45, No. 497, pp. 666-670.
- (24) Stuart P. Keeler, New Way to Select Material, Die Variables and Part Shape for Forming. Machinery, 1971, Vol. 77, No. 10, pp. 25-27.
- (25) Roger Pearce, A Users' Guide to Forming Limit Diagrams. Sheet Metal Industries, 1971, Vol. 48, No. 12, pp. 943-949.
- (26) J.L. Duncan, Measurement of Strain Hardening in Sheet Metals. Sheet Metal Industries, 1967, Vol. 44, No. 483, pp. 482-489.
- (27) C. CHR. Veerman & P.F. Neve, Some Aspects of the Determination of the Forming Limit Diagram (FLD) - Onset of Localized Necking. Sheet Metal Industries, 1972, Vol. 49, No. 6, pp. 421-423.
- (28) Stuart P. Keeler, Determination of Forming Limits in Automotive Stampings. Sheet Metal Industries, 1965, Vol. 42, No. 461, pp. 683-691.
- (29) L. Lilet, Suitability of Sheets for Pressing. Sheet Metal Industries, 1966, Vol. 43, No. 476, pp. 949-957.
- (30) Materials' Working Group of the International Deep Drawing Research Group (I.D.D.R.G.), The Plastic Anisotropy Ratio ' $r$ ' and The Work-Hardening Exponent ' $n$ ' in Relation to the Drawability of Sheet Metal. Sheet Metal Industries, 1967, Vol. 44, No. 484, pp. 523-532.

- (31) C. CHR. VEERMAN, L. HARTMAN, J.J. PEELS, P.F. NEVE, Determination of Appearing and Admissible Strains in Cold-Reduced Sheets. Sheet Metal Industries, 1971, Vol. 48, No. 9, pp. 678-680 and 692-694.
- (32) R. Pearce, The Tensile Test as a Guide to Sheet-Forming Properties. Sheet Metal Industries, 1963, Vol. 40, No. 433, pp. 317-322.
- (33) Stuart P. Keeler, Understanding Sheet Metal Formability. Machinery, 1968, Vol. 74: No. 6, pp. 88 - 95. No. 7, pp. 94-101. No. 8, pp. 94-103. No. 9, pp. 92-99. No. 10, pp. 98-104. No. 11, pp. 78-83.
- (34) Roger Pearce, An Introduction to the Sheet-Metal Forming Processes. Sheet Metal Industries, 1964, Vol. 41, No. 447, pp. 567-570.
- (35) Stuart P. Keeler, Some Variables that affect Metal Forming. Machinery, 1969, Vol. 75, No. 6, pp. 111-112 & 118.
- (36) Stuart P. Keeler, Circular Grid System - A valuable Aid for Evaluating Sheet-Metal Formability. Sheet Metal Industries, 1968, Vol. 45, No. 497, pp. 633-641.
- (37) Derek R. Palmer, Electro-Chemical Marking of Grids in Auto-Body Press Working. Sheet Metal Industries, 1968, Vol. 45, No. 491, pp. 198-204.
- (38) Stuart P. Keeler, Letter to the Editor Regarding Reference 37 above. Sheet Metal Industries, 1968, Vol. 45, No. 497, pp. 649-650.
- (39) Roger Pearce & I.C. Drinkwater, some Aspects of Electro-Chemical Marking. Sheet Metal Industries, 1968, Vol. 45, No. 498, pp. 751-755.
- (40) R. Pearce & J. Woodthorpe, an Aid to Practical Sheet Metal Forming. Journal of Mechanical Engineering Science, 1970, Vol. 12, No. 6, pp. 443-445.

- (41) J. Willis and J.C. Blade, A Proposed Earing Test For Sheet Metal. Sheet Metal Industries, 1966, Vol. 43, No. 468, pp. 316-320.
- (42) 'Impossible' Deep Draws/Made with New Steel. Machine Design, 1970, Vol. 42, No. 27, p. 10.
- (43) Product Data Bulletin, C-16 - Armco I.F. Steels. Armco Steel Corporation, Middletown, Ohio, U.S.A.